A Local Model for the Spherical Collapse/Expansion Problem

Elliot M Lynch, Guillaume Laibe

Monthly Notices of the ROYAL ASTRONOMICAL SOCIETY

MNRAS **524,** 1710–1726 (2023) https://doi.org/10.1093/mnras/stad1988
Advance Access publication 2023 July 3

A local model for the spherical collapse/expansion problem

Elliot M. Lynch★ and Guillaume Laibe

Univ Lyon, Univ Lyon1, Ens de Lyon, CNRS, Centre de Recherche Astrophysique de Lyon UMR5574, F-69230, Saint-Genis,-Laval, France

Accepted 2023 June 16. Received 2023 June 16; in original form 2022 December 8

ABSTRACT

Spherical flows are a classic problem in astrophysics which are typically studied from a global perspective. However, much like with accretion discs, there are likely many instabilities and small scale phenomena which would be easier to study from a local perspective. For this purpose, we develop a local model for a spherically contracting/expanding gas cloud, in the spirit of the shearing box, β-plane, and expanding box models which have had extensive use in studies of accretion discs, planets, and stellar winds, respectively. The local model consists of a, spatially homogeneous, periodic box with a time varying aspect ratio, along with a scale factor (analogous to that in FRW/Newtonian cosmology) relating the box coordinates to the physical coordinates of the global problem. We derive a number of symmetries and conservation laws exhibited by the local model. Some of these reflect symmetries of the periodic box, modified by the time dependant geometry, while others are local analogues for symmetries of the global problem. The energy, density, and vorticity in the box also generically increase(/decrease) as a consequence of the collapse(/expansion). We derive a number of non-linear solutions, including a local analogue of uniform density zonal flows, which grow as a consequence of angular momentum conservation. Our model is closely related to the accelerated expanding box model of Tenerani & Velli and is an extension of the isotropic model considered by Robertson & Goldreich.

Key words: hydrodynamics – methods: analytical – stars: formation – stars: winds, outflows.

1 INTRODUCTION

Spherically expanding/collapsing flows are a classic problem are a classic problem in astrophysics. Such flows include the classic Bondi spherical accretion problem Bondi (1952); the von Neumann–Sedov–Taylor solution for a spherical shock wave, used as a model of supernova explosions Sedov (1946); Taylor (1946, 1950); Bethe et al. (1958); solar and stellar winds (Velli, Grappin & Mangeney 1992; Grappin, Velli & Mangeney 1993; Grappin & Velli 1996; Tenerani & Velli 2017; Shi et al. 2020; Huang et al. 2022) and the spherical collapse problem (Larson 1969; Penston 1969; Hunter 1977; Shu 1977; Foster & Chevalier 1993) important for star and planet formation. While in many of these problems the spherically symmetric flow provides a useful approximation to the leading order dynamics, one expects there to be local departure from spherical symmetry that could be important in many applications. This is particularly true of the collapse problem as rotational flows are expected to grow during the collapse due to conservation of angular momentum (see also Velli et al. (1992); Grappin et al. (1993); Grappin & Velli (1996); Tenerani & Velli (2017); Shi et al. (2020); Huang et al. (2022) for an application where local flows are important in an expanding flow).

One can study local departures from the axisymmetric flows in the global picture, such as by performing full 3D simulations of the expansion/collapse. However it can be prohibitively computationally expensive to resolve both the scale of interest, while simulating the entire spherical expansion/collapse. Instead one can turn to local models, which are commonly used in astrophysics and planetary sciences to tackle such problems. Commonly used local models include the shearing box model (Goldreich & Lynden-Bell 1965; Hawley, Gammie & Balbus 1995; Latter & Papaloizou 2017), used in the study of accretion discs; the β-plane model Rossby (1939), used to study rotating planets; and, of particular relevance to our study here, the Expanding Box Model (EBM; Velli et al. 1992; Grappin et al. 1993; Grappin & Velli 1996) and Accelerated Expanding Box (AEB; Tenerani & Velli 2017), used to study stellar winds and the FRW like model of Robertson & Goldreich (2012) used to study turbulence in cosmological (i.e. homogeneous and isotropic) collapses. Such local models have had a number of notable successes in astrophysics, the most famous of which is the (re-)discovery of MRI by Hawley et al. (1995).

Of the existing local model the most relevant to our work is the EBM model for stellar winds, developed by Velli et al. (1992); Grappin et al. (1993); Grappin & Velli (1996). This model follows a local box in a (supersonic), uniformly, expanding magnetohydrodynamic (MHD) flow to study local instabilities and waves in the outer regions of solar and stellar winds. In this paper we are interested in deriving an expanding box like model valid for both radially and temporally varying spherical flows. The generalization of the EBM to radially varying flows was done in Tenerani & Velli (2017). The generalization to background flows which are also time dependant, motivated by the stellar formation problem, results in a model close to the AEB (although our treatment of pressure will be closer to the distorted shearing box models of Ogilvie & Latter (2013); Ogilvie & Barker (2014)). We shall focus, in this paper, on the hydrodynamic case as it posses a number of important features that are worth understanding before generalizing to MHD.

★ E-mail: elliot.lynch@ens-lyon.fr

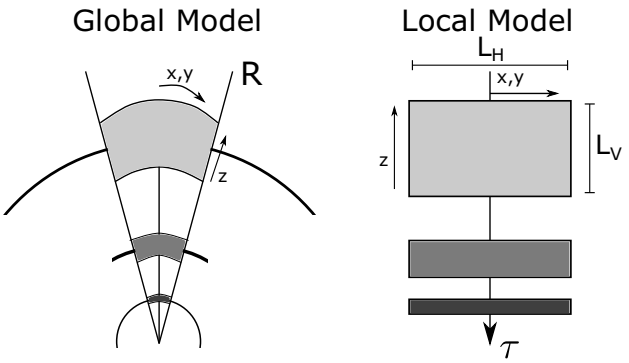

Figure 1. Geometry of the domain. Globally (left) the domain is bounded by radial shells which can approach or recede from each other depending on the gradients in the background velocity. Points within the domain move in the radial direction due to the spherically symmetric background flow. The local model (right) is a rectangular domain where the horizontal coordinates are equivalent to the latitude/longitude on the sphere and the vertical direction moves between spherical shells comoving with the background flow. The aspect ratio of this local box changes as the distance between the spherical shells varies.

In Section 2, we present the derivation of our local model. Sections 2.4 and 2.5 derives symmetries and conservation laws of the local model. Section 3 presents some non-linear solutions to the local model – and discuss how these relate to the global problem. In Section 4, we derive the linear theory of our local model. We discuss possible extension of our model in Section 5. We present our conclusions in Section 6 and additional mathematical details (including alternative formulations which maybe more convenient for implementation in hydrocodes) are presented in the appendices.

2 DERIVATION

2.1 Global geometry

To derive a local model for spherical collapse/expansion consider a local neighbourhood of a point, o, located on the equator of a sphere of radius R. The line element of the usual spherical polar coordinate system is

$$\mathrm{d}s^2 = \mathrm{d}R^2 + R^2(\mathrm{d}\theta^2 + \sin^2\theta\,\mathrm{d}\phi^2). \tag{1}$$

We are interested in describing the local dynamics near to p occurring on a horizontal length-scale $L_\mathrm{H} \ll R$ (See Fig. 1, which show the relationship between the global and local geometries). Without loss of generality, we can locate our local model on the equator of the sphere ($\theta = \pi/2$) meaning we can approximate the line element by

$$\mathrm{d}s^2 = \mathrm{d}R^2 + R^2(\mathrm{d}\theta^2 + \mathrm{d}\phi^2) + \mathcal{O}((L_\mathrm{H}/R)^2 d\phi^2), \tag{2}$$

which results in metric tensor components,

$$g_{RR} = 1, \quad g_{\theta\theta} = g_{\phi\phi} = R^2, \tag{3}$$

and inverse metric tensor components

$$g^{RR} = 1, \quad g^{\theta\theta} = g^{\phi\phi} = R^{-2}, \tag{4}$$

with all other components zero. The Christoffel symbols components, for this coordinate system, are

$$\begin{aligned}\Gamma^R_{\theta\theta} &= \Gamma^R_{\phi\phi} = -R,\\ \Gamma^\theta_{\theta R} &= \Gamma^\theta_{R\theta} = \Gamma^\phi_{\phi R} = \Gamma^\phi_{R\phi} = R^{-1},\end{aligned} \tag{5}$$

with all others vanishing. The fluid equations in this coordinate system are

$$Du^\theta + \frac{2}{R}u^R u^\theta = -R^{-2}\left(\partial_\theta\Phi + \frac{1}{\rho}\partial_\theta p\right), \tag{6}$$

$$Du^\phi + \frac{2}{R}u^R u^\phi = -R^{-2}\left(\partial_\phi\Phi + \frac{1}{\rho}\partial_\phi p\right), \tag{7}$$

$$Du^R - Ru^\phi u^\phi - Ru^\theta u^\theta = -\left(\partial_R\Phi + \frac{1}{\rho}\partial_R p\right), \tag{8}$$

$$D\rho = -\rho R^{-2}\partial_i(R^2 u^i), \tag{9}$$

where the Lagrangian derivative is

$$D = \partial_t + u^i\partial_i. \tag{10}$$

Note, we have listed the R component of the momentum equation last as it will become the z momentum equation in the local coordinate system. To close this system of equations, we must supplement them with an equation of state determining p, which we assume is barotropic,

$$p = p(\rho). \tag{11}$$

2.2 Spherical collapse/expansion

For the background fluid flow we wish to consider a spherically symmetric expanding/contracting fluid in a (potentially time dependant) central potential $\Phi = \Phi(t, R)$. Consider a spherically symmetric fluid in this potential with density $\rho_0 = \rho_0(R, t)$ and purely radial velocity field $U^i = U(R, t)\hat{e}^i_R$. The density of the fluid then evolves according to the continuity equation,

$$D_0\rho_0 = -\rho_0 R^{-2}\partial_R(R^2 U), \tag{12}$$

where the Lagrangian derivative of the background flow D_0 is given by,

$$D_0 = \partial_t + U\partial_R. \tag{13}$$

The radial momentum equation for the background flow determines how $U(R, t)$ evolves,

$$D_0 U = -\partial_R\Phi - \frac{1}{\rho_0}\partial_R p_0, \tag{14}$$

where $p_0 = p(\rho_0)$ is the fluid pressure. Spherical symmetry ensures that the θ and ϕ components of the momentum equation are satisfied.

This background flow naturally sets a characteristic time-scale, $t_\mathrm{bg} \sim R/|U|$, which is the time-scale over which the background flow evolves (in the AEB model of Tenerani & Velli (2017) their expansion time-scale τ_e is equal to our t_bg). In the collapse case we also have t_collapse (typically $\sim t_\mathrm{bg}$), which is the time-scale for the completion of the collapse (e.g. the free-fall time or $t_\mathrm{collapse} \sim t_\mathrm{bg} \sim \frac{R(0)}{c_s}$ in the isothermal sphere model of Shu (1977)). In general one expects t_bg to evolve with the background flow, typically getting longer in expanding flows and shorter for collapses.

2.3 Deriving the local model

The local model we shall derive is similar to the AEB (Tenerani & Velli 2017), however, we allow for a time dependant background flow and our treatment of pressure is closer to the distorted shearing box models of Ogilvie & Latter (2013); Ogilvie & Barker (2014). We are also interested in what happens when such a model is run in reverse as a model of a spherical collapse.

Consider local, non-linear, perturbations to the background, spherically symmetric, flow. We now write the fluid motion as the sum of

the background spherical collapse/expansion and a relative velocity v^i:

$$u^i = U\hat{e}^i_R + v^i. \tag{15}$$

The fluid dynamical equations for the relative velocity are, without approximation,

$$Dv^\theta + \frac{2}{R}(U+v^R)v^\theta = \frac{1}{\rho_0 R^2}\partial_\theta p_0 - \frac{1}{\rho R^2}\partial_\theta p, \tag{16}$$

$$Dv^\phi + \frac{2}{R}(U+v^R)v^\phi = \frac{1}{\rho_0 R^2}\partial_\phi p_0 - \frac{1}{\rho R^2}\partial_\phi p, \tag{17}$$

$$Dv^R + v^R\partial_R U - Rv^\phi v^\phi - Ru^\theta u^\theta = \frac{1}{\rho_0}\partial_R p_0 - \frac{1}{\rho}\partial_R p, \tag{18}$$

$$D\rho = -\rho[\Delta + R^{-2}\partial_i(R^2 v^i)], \tag{19}$$

where the Lagrangian derivative is

$$D = \partial_t + U\partial_R + v^i\partial_i, \tag{20}$$

and we have introduced the velocity divergence of the background flow,

$$\Delta = R^{-2}\partial_R(R^2 U). \tag{21}$$

As the fluid is barotropic, we can introduce the pseudo-enthalpy $h(\rho) = \int p(\rho) d\rho^{-1}$, and the momentum equations can now be written as

$$Dv^\theta + \frac{2}{R}(U+v^R)v^\theta = -\frac{1}{R^2}\partial_\theta h, \tag{22}$$

$$Dv^\phi + \frac{2}{R}(U+v^R)v^\phi = -\frac{1}{R^2}\partial_\phi h, \tag{23}$$

$$Dv^R + v^R\partial_R U - Rv^\phi u^\phi - Ru^\theta u^\theta = -\partial_R h - \partial_R h_0, \tag{24}$$

where $h_0 = h(\rho_0)$.

We are interested in describing local, non-linear, perturbations occurring on a horizontal length-scale $L_\mathrm{H} \ll R$ and vertical length-scale $L_\mathrm{V} \ll R$, where the non-linear curvature terms ($\frac{2}{R}v^R v^\phi$, $\frac{2}{R}v^R v^\theta$, $R(v^\phi v^\phi + v^\theta v^\theta)$) can be neglected at leading order. For a hypersonic collapse/expansion these terms are subdominant relative to the global curvature terms $\frac{2U}{R}$ and the vertical advection of the background flow, $v^R U_{0R}$ (assuming $U_{R0} \sim U/R$). This is the regime considered in the EBM of Velli et al. (1992); Grappin et al. (1993); Grappin & Velli (1996).[1] It also results in a similar asymptotic ordering scheme to that used to derive the shearing box (in particular the 'distorted' eccentric and warped variants, Ogilvie & Latter (2013); Ogilvie & Barker (2014)). However, typical collapse profile (such as Shu 1977) start out subsonic and transition to a hypersonic flow at late times and one would ideally like our local model to be able to handle this situation. In the highly subsonic regime, the local flows primarily consist of sound and vortical waves and the local model is (at leading order) a Cartesian, periodic, box with an anisotropic sound speed. The main influence of the background flow on the model, in this regime, is the slow variation of the horizontal and vertical sound speed with time. Thus the non-linear curvature term is subdominant to the terms involving pressure gradients.

In general then, in order that we can neglect the non-linear curvature terms we require

$$Rv^R v^\phi \ll \max(v^\phi RU, (L_\mathrm{H}/R)^{-1}c_s^2), \tag{25}$$

$$Rv^R v^\theta \ll \max(v^\theta RU, (L_\mathrm{H}/R)^{-1}c_s^2), \tag{26}$$

$$R(v^\phi v^\phi + v^\theta v^\theta) \ll \max(v^R RU_{R0}, (L_\mathrm{V}/R)^{-1}c_s^2). \tag{27}$$

To ensure that these terms are subdominant to either the terms involving the pressure gradient or the terms involving the background flow.

This requirement that the non-linear curvature terms be negligible tends to introduce a time-scale, t_curv, over which the local approximation is valid and time-scales longer than t_curv the neglected terms cause a significant departure from the predictions of the local model. This is particularly true for the collapse case ($U < 0$) as the non-linear curvature terms are expected to grow with time, eventually violating Conditions equations (25)–(27). This just reflects the expectation that (hydrodynamic) collapses tend to be halted when they achieve sufficient rotational support. Thing are easier for spherical expansions as the neglected terms tend to get smaller with the expansion. If $t_\mathrm{curv} \gtrsim t_\mathrm{collapse} \sim t_\mathrm{bg}$ then we can successfully employ the local model over most of the collapse. However when $t_\mathrm{curv} < t_\mathrm{collapse} \sim t_\mathrm{bg}$ our model breaks down before the collapse completes. While this is a limitation of the local model it's worth noting that physically if $t_\mathrm{curv} < t_\mathrm{collapse}$ this means the background spherical collapse is also not valid on time-scales longer than t_curv as local/non-spherical perturbations have grown sufficiently non-linear to modify the background collapse.

In addition to the non-linear curvature terms, we must also consider how to deal with the background pressure gradient, $-\partial_R h_0$. In the small box limit that we are considering, this term is always subdominant relative to the main pressure gradient term $-\partial_R h$. In the hypersonic limit, this term is also subdominant to the background advection terms and it is evident that one can neglect this term. The hypersonic limit (neglecting the $-\partial_R h_0$ term) is a consistent asymptotic limit of the background flow similar to the 'small' compressible shearing box as described in Latter & Papaloizou (2017). It is less obvious what should be done in the subsonic limit as here the advection terms are also subdominant. Tenerani & Velli (2017) have argued that both the background pressure gradient and background advection terms should be maintained as they are of the same order. However, it has been found that keeping the pressure gradient terms leads to spurious instabilities such as unstable sound waves[2] (See Latter & Papaloizou 2017, for a discussion in the shearing box context). This may be a consequence of the fact the basic state of the local model including the background pressure gradient is incompatible with the imposition of periodic boundaries that are typically required for numerical applications. The advection terms, on the other hand, are a relatively benign subdominant term in the subsonic limit. In fact on can show that the effects of the advection in the subsonic limit are equivalent to their effects on short-wavelength waves in the hypersonic limit. Therefore the correct approach appears to be to neglect the background pressure gradient, but maintain

[1] There is a subtlety in the EBM as the uniform expansion means that $U_{R0} = 0$ so that, strictly, $R(v^\phi v^\phi + v^\theta v^\theta)$ cannot, in general, be neglected. In the expanding box application one is saved by the fact that v^ϕ, v^θ tend to get small with the expansion as a consequence of angular momentum conservation meaning if they are small enough initially the non-linear curvature terms should remain small throughout the expansion. This is not the case if one were to run the expanding box in reverse to model a uniform collapse and thus extra care must be taken in this instance.

[2] It's unclear whether the gradients in the background magnetic field in the model of Tenerani & Velli (2017) will lead to similar spurious instabilities in the magnetosonic waves.

the background advection terms, provided that the box is small enough.

Neglecting the non-linear curvature terms, and background pressure gradient, the equations simplify to

$$Dv^\theta + \frac{2}{R}Uv^\theta = -\frac{1}{R^2}\partial_\theta h, \tag{28}$$

$$Dv^\phi + \frac{2}{R}Uv^\phi = -\frac{1}{R^2}\partial_\phi h, \tag{29}$$

$$Dv^R + v^R\partial_R U = -\partial_R h, \tag{30}$$

$$D\rho = -\rho[\Delta + \partial_i v^i]. \tag{31}$$

Consider a reference point following the spherical flow, starting at an initial radius R_0, and angular coordinates $\theta = \pi/2$, $\phi = 0$ at $t = 0$. Let $\mathcal{R}(t)$ be the solution of $d\mathcal{R}(t)/dt = U(\mathcal{R}(t), t)$ subject to the initial condition $\mathcal{R}(0) = R_0$. Then the coordinates of the reference point are $(\mathcal{R}(t), \theta, \phi) = (R_0, \pi/2, 0)$. We now consider a local neighbourhood of the reference point

$$\theta = \pi/2 + x, \quad \phi = y, \quad R = \mathcal{R}(t) + z, \quad t = \tau, \tag{32}$$

where x, y are $\mathcal{O}(L_\mathrm{H}/\mathcal{R})$, and z is $\mathcal{O}(L_\mathrm{V}/\mathcal{R})$ in our units. Thus our coordinate system consists of a (small) rectangular domain on the equator of a sphere of radius $\mathcal{R}$, with x, y being Cartesian coordinate describing the location of the point on this sphere and z denoting the height above the reference sphere along lines of radius. The radius of the reference sphere is then free to change with time – accounting for the spherical collapse/expansion in the global system.

Because of it's appearance in the Lagrangian derivative we must expand the background velocity vertically as follows

$$U = U_0(\tau) + U_{R0}(\tau)z. \tag{33}$$

All other geometrical/background quantities are evaluated at the reference point and are thus functions of time only.

Because of the time dependence of the coordinate system the old and new time derivatives are related by

$$\partial_t + U_0\partial_R = \partial_\tau, \tag{34}$$

while the Lagrangian time derivative is

$$D = \partial_t + U_{R0}z\partial_z + v^i\partial_i. \tag{35}$$

The resulting fluid equations in this coordinate system are then

$$Dv^x + \frac{2U_0}{\mathcal{R}}v^x = -\frac{1}{\rho\mathcal{R}^2}\partial_x p, \tag{36}$$

$$Dv^y + \frac{2U_0}{\mathcal{R}}v^y = -\frac{1}{\rho\mathcal{R}^2}\partial_y p, \tag{37}$$

$$Dv^z + v^z U_{R0} = -\frac{1}{\rho}\partial_z p, \tag{38}$$

where $p = p(\rho)$ is given by the barotropic equation of state. One drawback of the above coordinate system is that, excepting for the case of a uniformly contracting/expanding fluid, there is an explicit dependence on the vertical coordinate through the Lagrangian time derivative. This makes it harder to setup boundary conditions in the vertical direction. Similar to local models of distorted discs (e.g. Ogilvie & Barker 2014), we can rectify this deficiency by adopting a Lagrangian or Stretched vertical coordinate $\tilde{z} = z/L_z(\tau)$. $\tilde{z}$ is a Lagrangian coordinate with respect to the background flow, that is, $D_0\tilde{z} = 0$, where $D_0 = \partial_\tau + U_{R0}z\partial_z$. L_z is a characteristic vertical length-scale which encompasses the vertical stretching/compression of the fluid flow due to radial variations of the background velocity U. L_z evolves according to

$$\frac{dL_z}{d\tau} = U_{R0}L_z, \tag{39}$$

In principle, one can rescale the vertical coordinate such that $L_z(0) = R_0$. However, taking $L_z(0) = L_{z0}$, which need not equal R_0, allows for the exploration of flows with different horizontal and vertical length-scales.

The vertical partial derives are related by $\partial_z = L_z^{-1}\partial_{\tilde{z}}$ and the vertical velocities are related by $v^{\tilde{z}} = L_z^{-1}v^z$. Upon adopting the stretched vertical coordinates the Lagrangian time derivative transforms to a spatially homogeneous form,

$$D = \partial_\tau + v^x\partial_x + v^y\partial_y + v^{\tilde{z}}\partial_{\tilde{z}}. \tag{40}$$

The Jacobian determinant of the new coordinate system is $J = L_z\mathcal{R}^2$ and the coordinate system has the following line element

$$ds^2 = \mathcal{R}^2(\tau)[dx^2 + dy^2] + L_z^2(\tau)d\tilde{z}^2. \tag{41}$$

This choice of vertical coordinate puts the vertical and horizontal coordinates on equal footing. Both are dimensionless variables with an associated length-scale (L_z and $\mathcal{R}$, respectively). Using the relationship between $\mathcal{R}$ and U_0, along with equation (39) we can write Δ in terms of the time derivative of the Jacobian,

$$\Delta = \frac{2U_0}{\mathcal{R}} + U_{R0} = \frac{2}{\mathcal{R}}\frac{d\mathcal{R}}{d\tau} + \frac{1}{L_z}\frac{dL_z}{d\tau} = \frac{1}{J}\frac{dJ}{d\tau}. \tag{42}$$

In the stretched coordinate system the momentum and continuity equations of the local model are

$$Dv^x + \frac{2U_0}{\mathcal{R}}v^x = -\frac{1}{\rho\mathcal{R}^2}\partial_x p, \tag{43}$$

$$Dv^y + \frac{2U_0}{\mathcal{R}}v^y = -\frac{1}{\rho\mathcal{R}^2}\partial_y p, \tag{44}$$

$$Dv^{\tilde{z}} + 2v^{\tilde{z}}U_{R0} = -\frac{1}{\rho L_z^2}\partial_{\tilde{z}} p, \tag{45}$$

$$D\rho = -\rho\left[\Delta + \partial_x v^x + \partial_y v^y + \partial_{\tilde{z}} v^{\tilde{z}}\right]. \tag{46}$$

equations (43)–(46) form our local model. As explored in subsequent sections, one unusual property of this model, that can be deduced from the form of these equations, is the differing effective sounds speeds for sound waves propagating in the vertical and horizontal directions when $L_z \neq \mathcal{R}$.

Alternatively, the momentum equation can be written in terms of the covariant velocity, v_i, which are in many ways simpler,

$$Dv_x = -\frac{1}{\rho}\partial_x p, \tag{47}$$

$$Dv_y = -\frac{1}{\rho}\partial_y p, \tag{48}$$

$$Dv_{\tilde{z}} = -\frac{1}{\rho}\partial_{\tilde{z}} p. \tag{49}$$

Notably this implies conservation of the generalized momenta, ρv_i.

With this choice of coordinate systems we can now use reflective/closed boundaries (for no mass/momentum flux with neighbouring radial shells) or periodic boundaries in the vertical direction. In the horizontal direction, periodic boundaries are the physically meaningful boundary conditions as these allow use to consider the behaviour of high-m perturbations to spherical flows in a local model. The possibility to use periodic boundaries significantly simplify numerical implementation of the model.

A more general choice of boundary condition which will allow for the study of a much wider class of flows is to adopt shear-periodic boundary conditions analogous to those seen in shearing

box models, provided the shear across the box is not too large such that the curvature terms become important. Using shear periodic boundary conditions likely allows for the modelling of a weakly rotating collapse/expansion within the local framework. A proper exploration of the shear-periodic local model and it's correspondence with a weakly rotating spherical flows is beyond the scope of this paper and will be left for future work.

The local model can be derived from the following Lagrangian density

$$\mathcal{L} = \rho_0 \left[\frac{1}{2}\mathcal{R}^2(v^x v^x + v^y v^y) + \frac{1}{2} L_z^2 v^{\tilde{z}} v^{\tilde{z}} - \varepsilon \right], \tag{50}$$

where ε is the specific internal energy.

We can also reformulate the local model in terms of a FRW like metric:

$$ds^2 = a^2(\tau)[dx^2 + dy^2 + b^2(\tau')d\tilde{z}^2], \tag{51}$$

where a is the scale factor and b the box aspect ratio. One has the choice to absorb the dimensions into the scale factor or the coordinate system. a and b are related to $\mathcal{R}$ and L_z through

$$a = \mathcal{R}, \quad b = L_z/\mathcal{R}. \tag{52}$$

This leads to the following fluid equations

$$Dv^x + 2Hv^x = -\frac{a^{-2}}{\rho}\partial_x p, \tag{53}$$

$$Dv^y + 2Hv^y = -\frac{a^{-2}}{\rho}\partial_y p, \tag{54}$$

$$Dv^{\tilde{z}} + 2Hv^{\tilde{z}} + 2\frac{\dot{b}}{b}v^{\tilde{z}} = -\frac{a^{-2}b^{-2}}{\rho}\partial_{\tilde{z}} p, \tag{55}$$

$$D\rho = -\rho\left[3H + \frac{\dot{b}}{b} + \partial_x v^x + \partial_y v^y + \partial_{\tilde{z}} v^{\tilde{z}}\right], \tag{56}$$

where we have defined the Hubble parameter $H = \dot{a}/a$. For a constant aspect ratio box, $\dot{b} = 0$, these equations are equivalent to Robertson & Goldreich (2012). Various alternative formulations of the local model, of potential use for numerical implementations, are given in Appendix A. Of note is the time dependant background terms in the continuity equation, and in front of the pressure gradients, can be absorbed into a time dependant, anisotropic, and effective sound speed.

2.4 Symmetries of the local model

Ideal gas dynamics has a number of important symmetries, such as Galilean transforms, rotations, and length-scale, time-scale, and mass rescaling. The global problem similarly has many symmetries – in particular global rotational symmetries along with the choice of rotating frame. One would also expect that many of these symmetries should be reflected in the local model. In this section we shall explore which of these symmetries are carried over/modified in the local model.

Fluid dynamics in periodic, Cartesian boxes are invariant under Galilean transforms. In the local model, one expect such Galilean transforms will be modified by the time dependant geometry. Consider a modified Galilean transform where the new position and time-scale are related to the old ones by

$$\mathbf{x}' = \mathbf{x} - \int \mathbf{v}_g(\tau)d\tau, \quad \tau' = \tau, \tag{57}$$

where $\mathbf{v}_g(t)$ is the new frame velocity which is uniform across the box, but can undergo acceleration. The velocity transforms according to

$$\mathbf{v}' = \mathbf{v} - \mathbf{v}_g. \tag{58}$$

This results in partial derivatives which transform according to

$$\partial_\tau = \partial'_\tau - v_g^i \partial_i, \quad \partial_x = \partial'_x. \tag{59}$$

The Lagrangian time derivative is unchanged by this transform with $D = \partial'_t + v^{i'}\partial'_i$, similarly the divergence of the relative velocity is left unchanged ($\partial_i v^i = \partial'_i v^{i'}$). This means the continuity equation is unchanged by the transform. In order for the momentum equations to remain unchanged by this transform we require that the frame velocity, $\mathbf{v}_g$, satisfy

$$\dot{v}_g^x + \frac{2U_0}{\mathcal{R}} v_g^x = 0, \tag{60}$$

$$\dot{v}_g^x + \frac{2U_0}{\mathcal{R}} v_g^y = 0, \tag{61}$$

$$\dot{v}_g^{\tilde{z}} + 2U_{R0} v_g^{\tilde{z}} = 0. \tag{62}$$

We see that during a collapse ($U_0 < 0$), horizontal frame translations accelerate with time in order to conserve angular momentum in the global frame. These horizontal translations in the local frames thus correspond to a (slow) global rotation of the reference sphere. The vertical frame translation correspond to a acceleration of the reference sphere relative to the background flow – that is, the reference sphere falls/rises at a slightly faster/slower rate than the background flow.

Ideal gas dynamics in Cartesian geometry exhibit a similarity transform where the dynamics are invariant under rescaling of the length-/time-scale. The local model exhibits a similar similarity transform, however here we must be careful to also perform an appropriate rescaling of the background flow. Consider a rescaling of space, time and fluid entropy by constant factors such that the length and time-scale transform like

$$\mathbf{x} \mapsto \lambda \mathbf{x}, \quad \tau \mapsto \mu\tau, \tag{63}$$

while (assuming a perfect gas) the pressure transforms like

$$p \mapsto \kappa p. \tag{64}$$

Under this rescaling, the partial derivatives transform according to

$$\partial_t \mapsto \mu^{-1}\partial_t, \quad \partial_i \mapsto \lambda^{-1}\partial_i, \tag{65}$$

and the velocity transforms according to

$$\mathbf{v} \mapsto \lambda\mu^{-1}\mathbf{v}. \tag{66}$$

This results in the Lagrangian time derivative transforming like $D \mapsto \mu^{-1}D$. This transformation works provided that the background flow is also transformed like

$$\mathcal{R} \mapsto (\kappa/\lambda)^{-1/2}\mathcal{R}, \quad L_z \mapsto (\kappa/\lambda)^{-1/2}L_z, \tag{67}$$

$$U_0 \mapsto (\kappa/\lambda)^{-1/2}\mu^{-1}U_0, \quad U_{R0} \mapsto \mu^{-1}U_{R0}. \tag{68}$$

This also results in $\Delta \mapsto \mu^{-1}\Delta$. This allows us to relate the local flows of two different, but homologous, spherical flows by a rescaling of the length-scale, time-scale and entropy of the local flow.

Independently of this similarity transform one can also rescale the vertical length-scale of the local model – corresponding to changing the aspect ratio of the box. Consider a rescaling of the vertical length-scale, L_z, by a constant factor r with $L_z \mapsto r^{-1}L_z$. If we simultaneously rescale the stretched vertical coordinate by

$$\tilde{z} \mapsto r\tilde{z}, \tag{69}$$

then as, physical vertical coordinate $z = \tilde{z}L_z$ is left unchanged by this transform, the dynamics are unchanged by this rescaling, that is, if we rescale L_z by a constant factor then the local dynamics are left unchanged if we simultaneously rescale the vertical extent of the box. Under this change of aspect ratio the vertical partial derivative transforms as $\partial_{\tilde{z}} \mapsto r^{-1}\partial_{\tilde{z}}$, while the vertical velocity transforms according to

$$v^{\tilde{z}} \mapsto r v^{\tilde{z}}, \tag{70}$$

meaning D is unchanged by this change of aspect ratio. One consequence of this rescaling, however, is the velocity field in the new coordinate system may posses shear where the original contained none. This will be particularly important to the diagonally propagating sound waves discussed in subsequent section.

Finally the local model is invariant under mass rescaling ($\rho \mapsto \lambda\rho$, $p \mapsto \lambda p$), assuming a perfect gas, and horizontal rotations. Unlike fluid dynamics in a periodic, Cartesian, box, the local model is not symmetric to rotations in the vertical direction unless the aspect ratio of the box is fixed ($L_z \propto \mathcal{R}$). This is a consequence of the different effective sound speed in the vertical and horizontal direction, along with the differing contributions from the background velocity.

2.5 Conservation laws

The conservative form of the continuity equation in the local model is

$$\partial_\tau(J\rho) + \partial_x(J\rho v^x) + \partial_y(J\rho v^y) + \partial_{\tilde{z}}(J\rho v^{\tilde{z}}) = 0 \quad . \tag{71}$$

In an ideal barotropic fluid, vorticity is a conserved tensor density which is related to the relabelling symmetries of ideal fluid Lagrangian (Padhye & Morrison 1996). The local model preserves this relabelling symmetry so we should expect the model to have a form of vorticity conservation. In the global coordinates the fluid vorticity obeys

$$\begin{aligned} \mathcal{D}\omega^i &= D\omega^i - \omega^j\nabla_j u^i + \omega^i\nabla_j u^j, \\ &= (\partial_t + u^i\partial_i)\omega^i - \omega^j\partial_j u^i + \omega^i\nabla_j u^j, \\ &= 0, \end{aligned} \tag{72}$$

where, in this paragraph only, $D = \partial_t + u^i\nabla_i$ is the Lagrangian time derivative with respect to the total (global + local) flow. The latter expression being a consequence of the symmetry of the Christoffel symbols. The vorticity depends only on the relative velocity as the background flow is irrotational,

$$\omega^i = \varepsilon^{ijk}\partial_j v_k \quad , \tag{73}$$

where ε^{ijk} is the volume element of the local model. Substituting equation (15), into equation (72), for the fluid velocity we obtain, in local (unstretched) coordinates,

$$\begin{aligned} &D\omega^i + \omega^i[\Delta + \partial_x v^x + \partial_y v^y + \partial_z v^z] - \omega^z U_{R0}\delta^i_z \\ &\quad - (\omega^x\partial_x + \omega^y\partial_y + \omega^z\partial_z)v^i = 0. \end{aligned} \tag{74}$$

Upon introducing the stretched vertical coordinate, $\tilde{z}$, this simplifies to

$$\begin{aligned} &D\omega^i + \omega^i[\Delta + \partial_x v^x + \partial_y v^y + \partial_{\tilde{z}} v^{\tilde{z}}] \\ &- (\omega^x\partial_x + \omega^y\partial_y + \omega^{\tilde{z}}\partial_{\tilde{z}})v^i = 0\,. \end{aligned} \tag{75}$$

It is informative to write the above in terms of the tensor density advection operator with respect to the relative flow, $\mathcal{D}_{\rm rel}$,

$$\mathcal{D}_{\rm rel}\omega^i = -\omega^i\Delta \quad , \tag{76}$$

where, when acting on the vorticity, the advection operator with respect to the background flow is

$$\mathcal{D}_{\rm rel}\omega^i = D\omega^i + \omega^i\partial_j v^j - \omega^j\partial_j v^i, \tag{77}$$

with $D = \partial_\tau + v^i\partial_i$ the usual Lagrangian time derivative in the local model. Thus we see that the change in box volume, through Δ, results in a source/sink of vorticity. In the global picture the vorticity is advected by the total flow, in the local picture the vorticity is advected by the relative flow with the background flow appearing as a source/sink. This is analogous to the situation in cosmology where the peculiar velocities redshift to zero in an expanding FRW metric resulting in $\omega_i \propto a^{-1}$ (Mo, Van den Bosch & White 2010). The closely related quantity, $J\omega^i$, is conserved by the local model, with no source/sink from the box volume change. The effect of the changing box volume on the fluid vorticity can be seen in the simulations of Robertson & Goldreich (2012) (where it is referred to as adiabatic heating), with a rapidly contracting box leading to a strengthening of large scale eddies and a corresponding increase in the turbulent velocities.

The kinetic helicity, H_k, is a conserved quantity associated with the vorticity which is conserved in barotropic ideal fluids. Despite the collapse/expansion acting as a source/sink of vorticity, one can show that the kinetic helicity of the relative flow is conserved. The kinetic helicity of the relative flow is

$$\begin{aligned} H_k &= \iiint v_i\varepsilon^{ijk}\partial_j v_k dV, \\ &= \iiint v_i\varepsilon^{ijk}\partial_j v_k J dx\,dy\,d\tilde{z}. \end{aligned} \tag{78}$$

Taking the time derivative of H_k,

$$\begin{aligned} \dot{H}_k &= \iiint \left(\dot{v}_i\varepsilon^{ijk}\partial_j v_k + v_i\varepsilon^{ijk}\partial_j\dot{v}_k\right) J dx\,dy\,d\tilde{z}, \\ &= -\iiint \Big[\left(v^a\partial_a v_i + \partial_i h\right)\varepsilon^{ijk}\partial_j v_k \\ &\quad + v_i\varepsilon^{ijk}\partial_j\left(v^a\partial_a v_k + \partial_k h\right)\Big] J dx\,dy\,d\tilde{z}, \\ &= -\iiint \partial_j\left(\varepsilon^{ijk}v_k v^a\partial_a v_i + \varepsilon^{ijk}v_k\partial_i h\right) J dx\,dy\,d\tilde{z}, \\ &= 0. \end{aligned} \tag{79}$$

where we have made use of the antisymmetry of ε^{ijk}, $\partial_t(\varepsilon^{ijk}J) = 0$, along with the periodic boundary conditions. Conservation of kinetic helicity in the local model is not surprising as the stretching due to the background flow is not able to change the flow topology in the box.

Unlike hydrodynamics in both Cartesian and spherical geometries, the local model does not posses time translation symmetry. One can still obtain an energy equation for the relative motion. The conservative form of the energy equation for the relative motion in the, stretched, local coordinates is

$$\begin{aligned} &\partial_\tau\left(J\rho\mathcal{E}_{\rm rell}\right) + \partial_i\left[Jv^i\left(\rho\mathcal{E}_{\rm rell} + p\right)\right] \\ &\quad = -J\rho\left[U_R L_z^2 v^{\tilde{z}}v^{\tilde{z}} + \frac{U_0}{\mathcal{R}}\mathcal{R}^2\left(v^x v^x + v^y v^y\right)\right] - Jp\Delta, \end{aligned} \tag{80}$$

where the energy of the relative motion is given by

$$\mathcal{E}_{\rm rell} = \frac{1}{2}L_z^2 v^{\tilde{z}}v^{\tilde{z}} + \frac{1}{2}\mathcal{R}^2(\tau)[v^x v^x + v^y v^y] + \varepsilon. \tag{81}$$

Thus we see that the background flow is a source/sink of energy for the local model, through the *pdV* work done by the flow, and through

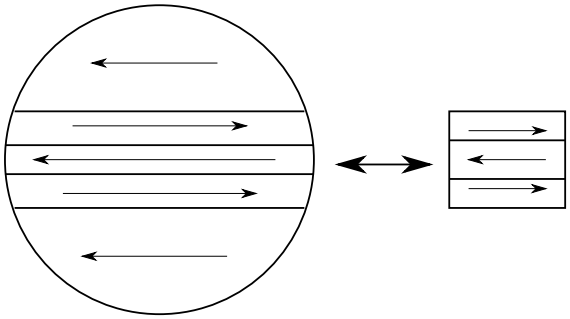

Figure 2. Horizontal shear flows in the local model are equivalent to (uniform density) zonal flows on the collapsing(/expanding) reference sphere in the global model.

the gradients in the background flow which are accessed through the Reynolds stresses. This is similar to the energy equations obtained in distorted shearing box models (e.g. Ogilvie & Barker 2014)

3 NON-LINEAR-SOLUTIONS

3.1 Horizontal shear flows

We can consider solutions to the local model with a spatially homogeneous density $\rho = \rho(\tau)$ and a purely horizontal velocity field ($v^z = 0$) of the form

$$v^i = A(t) v_0(\tilde{z}, \lambda) \hat{v}^i(\tilde{z}), \tag{82}$$

where $\lambda = \hat{v}^y(\tilde{z})x - \hat{v}^x(\tilde{z})y$. This flow consists of a horizontal shear flow that is uniform along the flow direction, $\hat{\mathbf{v}}$, but can vary perpendicular to $\hat{\mathbf{v}}$. This result in shear across these perpendicular directions. We set $A = 1$ at some initial time $\tau = \tau_0$, so that $v_0(\tilde{z}, \lambda)\hat{v}^i(\tilde{z})$ represents the initial velocity field in the fluid.

Note that we have

$$\begin{aligned} \partial_x v^x + \partial_y v^y &= A\left(\hat{v}^x \partial_x v_0 + \hat{v}^y \partial_y v_0\right) \\ &= A\left(\hat{v}^x \hat{v}^y \partial_\lambda v_0 - \hat{v}^y \hat{v}^x \partial_\lambda v_0\right) \\ &= 0, \end{aligned} \tag{83}$$

meaning this velocity field doesn't cause a change in density, or pressure. Also, we have

$$\begin{aligned} D v_0 &= A v_0 \left(\hat{v}^x \partial_x v_0 + \hat{v}^y \partial_y v_0\right) \\ &= A v_0 \left(\hat{v}^x \hat{v}^y \partial_\lambda v_0 - \hat{v}^y \hat{v}^x \partial_\lambda v_0\right) \\ &= 0. \end{aligned} \tag{84}$$

Given the above expression, equation (82) is a solution to the local model provided that the amplitude A evolves according to

$$\dot{A} + \frac{2U_0}{\mathcal{R}} A. \tag{85}$$

Making use of $d\mathcal{R}/d\tau = U_0$ we find that

$$A = (\mathcal{R}/R_0)^{-2}, \tag{86}$$

yielding the following for the velocity field at time t

$$v^i = v_0(\tilde{z}, \hat{v}^y(\tilde{z})x - \hat{v}^x(\tilde{z})y)\hat{v}^i(\tilde{z})\,(\mathcal{R}/R_0)^{-2}. \tag{87}$$

This is the local manifestation of conservation of angular momentum in the zonal flows of the global model.

These represent stratified zonal flows, of constant density, in the global geometry (as illustrated in Fig. 2) which grow/attenuate due to conservation of angular momentum with a change in the size of the reference sphere. The orientation of these zonal flows is free to vary with height due to the absence of shear stress.

In a collapse, these zonal flows grow in strength with time. It is unlikely that the shear flow can steepen indefinitely without going unstable, likely by going Kelvin–Helmholtz unstable at the locations of maximum shear. This may result in zonal flows of approximately constant velocity separated by horizontal vortices/rolls. As the collapse proceeds still further these zonal flows will continue to strengthen. Whether the non-linear outcome of this collapse results in a disruption of the ordered vortex layer, zonal flow geometry into fully developed turbulence throughout the box, or in a reorientation of the zonal flows until they self-organize into a stable shear flow will require numerical simulation to determine.

Of course if the collapse is allowed to proceed indefinitely, the zonal flows will become so strong that they break the asymptotic scheme used to derive the local model. In the global model these zonal flows will ultimately grow strong enough to provided rotational support to the gas, slowing or halting the collapse.

3.2 Elevator flows

A second class of non-linear flows which can be supported by the local model are vertically homogeneous 'elevator flows' of constant density. These can only occur for periodic vertical boundaries, an appear to be analogous to the elevator flows seen in some unstratified disc simulations (e.g. Dewberry, Latter & Ogilvie 2019; Dewberry et al. 2020). Here the density, and pressure, is a function of time only $\rho = \rho(\tau)$. The horizontal velocities are zero, $v^x = v^y = 0$. The vertical velocity is given by,

$$v^{\tilde{z}} = B(\tau) v_0^{\tilde{z}}(x, y), \tag{88}$$

where $v_0^{\tilde{z}}$ is the vertical velocity at $\tau = \tau_0$. This works because $\partial_{\tilde{z}} v^{\tilde{z}} = 0$, meaning this velocity field results in no change in density, and $D v_0^{\tilde{z}} = v^{\tilde{z}} \partial'_{\tilde{z}} v_0^{\tilde{z}} = 0$. Substituting equation (88) into the vertical momentum equation we obtain the following equation for the evolution of B,

$$\dot{B} + 2BU_{R0} = 0. \tag{89}$$

Making use of $dL_z/d\tau = U_{R0}L_z$ we find that

$$B = (L_z/L_{z0})^{-2}, \tag{90}$$

yielding the following for the velocity field at time t,

$$v^{\tilde{z}} = v_0^{\tilde{z}}(x, y)(L_z/L_{z0})^{-2}. \tag{91}$$

This grows provided that $U_{R0} < 0$.

These elevator flows can only occur with vertically periodic boundaries, and do not occur for closed/reflective boundary conditions. Unlike the horizontal flows considered in Section 3.1, which are the local realization of zonal flows present in the global geometry, these vertical elevator flows may be an artefact of periodic boundaries. Similar elevator flows are found in simulations of accretion discs with vertically periodic boundaries, despite not being present in the global problem (Dewberry et al. 2019; Dewberry et al. 2020).

3.3 Diagonal flows

There are a set of diagonal flows of the form

$$v^x = (\mathcal{R}/R_0)^{-2} v_0^x(y), \tag{92}$$

$$v^{\tilde{z}} = (L_z/L_{z0})^{-2} v_0^{\tilde{z}}(y), \tag{93}$$

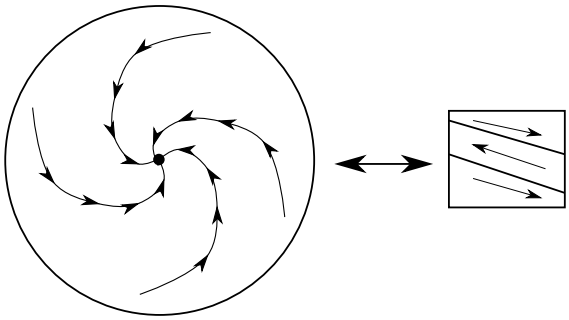

Figure 3. More generally these uniform density shear flows in the local model are local representations of a (weakly) differentially rotating flow with the streamlines in the global model spiralling towards/away from the centre of the sphere.

where, without loss of generality we can align the diagonal flow with the x-axis. Globally these flows represent a uniform density spiral in the global flow (as illustrated in Fig. 3) where the pitch angle of the spiral varies with 'latitude' on the reference sphere. As the vertical and horizontal velocities evolve separately the pitch angle of the spiral changes with time.

In general the horizontal shear, elevator and diagonal flows are local representations of weak departures from spherical symmetry in the global model. This is similar to the local representation of disc warps and eccentricity in (circular) shearing box (e.g. Balbus & Ricotti (1999); Latter & Ogilvie (2006); Ogilvie (2022)).

3.4 Other non-linear solutions

It is possible to find additional non-linear solutions; notably it appears to be possible to generalize homentropic/Kidda-like vortex solution for certain background flows. Additionally adopting shear periodic boundary allows for a more general class of shear flow than those considered here. We leave exploration of both of these classes of solution to future work as they are of interest in their own right.

4 LINEAR PERTURBATIONS

We now explore the behaviour of linear waves in the local model. For our background state we take $\rho = \rho(\tau)$ and $v^i = 0$, where

$$D\rho = -\rho\Delta, \tag{94}$$

with Δ the velocity divergence of the background flow. The linearized equations of motion and continuity, on top of this background state are

$$D\delta v^x + \frac{2U_0}{\mathcal{R}}\delta v^x = -\mathcal{R}^{-2}\partial_x\delta h \tag{95}$$

$$D\delta v^y + \frac{2U_0}{\mathcal{R}}\delta v^y = -\mathcal{R}^{-2}\partial_y\delta h \tag{96}$$

$$D\delta v^{\tilde z} + 2U_{R0}\delta v^{\tilde z} = -L_z^{-2}\partial_{\tilde z}\delta h \tag{97}$$

$$D\delta\rho = -\rho\partial_i\delta v^i - \delta\rho\Delta. \tag{98}$$

The enthalpy perturbation, δh, can be written in terms of the relative density perturbation $\delta\psi = \frac{\delta\rho}{\rho}$ through

$$\delta h = c_s^2\delta\psi. \tag{99}$$

The relative density perturbation evolves according to

$$D\delta\psi = -\partial_i\delta v^i. \tag{100}$$

Introducing a Lagrangian displacement (following Lynden-Bell & Ostriker 1967; Papaloizou 2005) of the form $\boldsymbol{\xi} = \hat{\boldsymbol{\xi}}\exp(i\mathbf{k}\cdot\mathbf{x})$ such that $\delta\mathbf{v} = D\boldsymbol{\xi}$ and the relative density perturbation which is related to the Lagrangian displacement by

$$\delta\hat\psi = -i\mathbf{k}\cdot\hat{\boldsymbol{\xi}}. \tag{101}$$

Substituting these into the linearized momentum equation we obtain

$$D^2\hat\xi^x + \frac{2U_0}{\mathcal{R}}D\hat\xi^x = -c_{sH}^2k_xk_i\hat\xi^i, \tag{102}$$

$$D^2\hat\xi^y + \frac{2U_0}{\mathcal{R}}D\hat\xi^y = -c_{sH}^2k_yk_i\hat\xi^i, \tag{103}$$

$$D^2\hat\xi^{\tilde z} + 2U_{R0}D\hat\xi^{\tilde z} = -c_{sV}^2k_{\tilde z}k_i\hat\xi^i. \tag{104}$$

The can be derived from the following Lagrangian density (which can alternatively be obtained from equation (50))

$$\mathcal{L} = \frac{1}{2}\mathcal{R}^2(\delta\hat v^x\delta\hat v^x + \delta\hat v^y\delta\hat v^y) + \frac{1}{2}L_z^2\delta\hat v^{\tilde z}\delta\hat v^{\tilde z} - \frac{1}{2}c_s^2(k_i\hat\xi^i)^2, \tag{105}$$

where, without loss of generality we can rotate the box such that $k_y = 0$. Variation with respect to $\hat{\boldsymbol{\xi}}$ leads to equations (102)–(104). Associated with this Lagrangian we have the Hamiltonian density

$$\mathcal{H} = \frac{1}{2}\mathcal{R}^{-2}(\hat\pi_x^2 + \hat\pi_y^2 + b^{-2}\hat\pi_{\tilde z}^2) + \frac{1}{2}c_s^2(k_i\hat\xi^i)^2, \tag{106}$$

where $\hat\pi_x = \mathcal{R}^2\delta\hat v^x$, $\hat\pi_y = \mathcal{R}^2\delta\hat v^y$, $\hat\pi_{\tilde z} = L_z^2\delta\hat v^{\tilde z}$ and we have made use of the aspect ratio $b = L_z/\mathcal{R}$. Performing a canonical transform using the following generating function

$$G = P_\alpha k_i\hat\xi^i + P_\beta(\aleph\hat\xi^x + \beth\hat\xi^{\tilde z}) + P_\gamma\hat\xi^y, \tag{107}$$

where $\aleph$ and $\beth$[3] are to be determined. This results in the following relationship between old and new coordinates and momenta,

$$\hat\pi_x = P_\alpha k_x + P_\beta\aleph \tag{108}$$

$$\hat\pi_y = P_\gamma, \tag{109}$$

$$\hat\pi_{\tilde z} = P_\alpha k_{\tilde z} + P_\beta\beth \tag{110}$$

$$\alpha = k_i\hat\xi^i, \tag{111}$$

$$\beta = \aleph\hat\xi^x + \beth\hat\xi^{\tilde z}, \tag{112}$$

$$\gamma = \hat\xi^y, \tag{113}$$

Consider the contribution to the Hamiltonian density from $\hat\pi_x^2 + b^{-2}\hat\pi_{\tilde z}^2$. Writing this in terms of the new momenta we obtain

$$\begin{aligned}\hat\pi_x^2 + b^{-2}\hat\pi_{\tilde z}^2 &= (P_\alpha k_x + P_\beta\aleph)^2 + b^{-2}(P_\alpha k_{\tilde z} + P_\beta\beth)^2\\ &= (k_x^2 + b^{-2}k_{\tilde z}^2)P_\alpha^2 + (\aleph^2 + b^{-2}\beth^2)P_\beta^2\\ &\quad + 2(\aleph k_x + k_{\tilde z}b^{-2}\beth)P_\alpha P_\beta.\end{aligned} \tag{114}$$

For boxes of constant aspect ratio we can diagonalize this by setting $\aleph k_x + k_{\tilde z}b^{-2}\beth = 0$, meaning the α, β, and γ linear perturbations are decoupled. In general choosing

$$\aleph = \frac{k_{\tilde z}}{\sqrt{k_x^2b_0^2 + k_{\tilde z}^2}}, \tag{115}$$

$$\beth = -\frac{k_xb_0^2}{\sqrt{k_x^2b_0^2 + k_{\tilde z}^2}}, \tag{116}$$

[3]The Hebrew letters aleph and beth

where we have introduced $b_0 = b(0)$, means that the dynamics of the α, β, and γ waves are initially independent, but changes to the box aspect ratio introduces a 'mixing' of the α and β waves. With this choice this leads to the following, transformed, Hamiltonian density:

$$\mathcal{H} = \frac{1}{2}\mathcal{R}^{-2}\Bigg\{(k_x^2 + b^{-2}k_{\tilde{z}}^2)P_\alpha^2 + \frac{k_x^2 b_0^2 (b/b_0)^{-2} + k_{\tilde{z}}^2}{k_x^2 b_0^2 + k_{\tilde{z}}^2} P_\beta^2 + 2\frac{k_{\tilde{z}}k_x}{\sqrt{k_x^2 b_0^2 + k_{\tilde{z}}^2}}[1 - (b/b_0)^{-2}]P_\alpha P_\beta + P_\gamma^2\Bigg\} + \frac{1}{2}c_s^2\alpha^2. \quad (117)$$

This Hamiltonian is independent of both β and γ, meaning P_β and P_γ are both constants of motion and β and γ satisfy

$$\dot{\beta} = \mathcal{R}^{-2}\frac{k_x^2 b_0^2 (b/b_0)^{-2} + k_{\tilde{z}}^2}{k_x^2 b_0^2 + k_{\tilde{z}}^2} P_\beta + \mathcal{R}^{-2}k_{\tilde{z}}k_x \frac{1 - (b/b_0)^{-2}}{\sqrt{k_x^2 b_0^2 + k_{\tilde{z}}^2}} P_\alpha, \quad (118)$$

$$\dot{\gamma} = \mathcal{R}^{-2}P_\gamma. \quad (119)$$

The latter just being a linear shear flow in the $y-$direction. P_β and P_γ can be related to the Fourier components of the vorticity perturbation, $\delta\omega^i$, through

$$\delta\omega^x = -\frac{ik_{\tilde{z}}}{J}P_\gamma, \quad (120)$$

$$\delta\omega^x = -\frac{i}{J}\sqrt{k_x^2 b_0^2 + k_{\tilde{z}}^2}P_\beta, \quad (121)$$

$$\delta\omega^{\tilde{z}} = \frac{ik_x}{J}P_\gamma. \quad (122)$$

The linearized form of equation (76) is $\partial_t(J\delta\omega^i) = 0$, so we see that P_β and P_γ being integrals of motion arises as a result of vorticity conservation. We can thus identify the (α, P_α) with the sound wave, while (β, P_β) and (γ, P_γ) are vortical waves. Changes in the box aspect ratio leads to coupling between the sound wave and the (β, P_β) vortical waves.

Treating P_β and P_γ as parameters, the Hamiltonian for the dynamics of (α, P_α) reduces to

$$\mathcal{H} = \frac{1}{2}\mathcal{R}^{-2}(k_x^2 + b^{-2}k_{\tilde{z}}^2)P_\alpha^2 + \mathcal{R}^{-2}k_{\tilde{z}}k_x\frac{1 - (b/b_0)^{-2}}{\sqrt{k_x^2 b_0^2 + k_{\tilde{z}}^2}}P_\alpha P_\beta + \frac{1}{2}c_s^2\alpha^2. \quad (123)$$

One can show that the dynamics of this system correspond to a forced harmonic oscillator with a variable frequency by switching the position and momenta,

$$\mathcal{H} = \frac{1}{2}\Pi^2 + \frac{1}{2}\omega^2 X^2 - g P_\beta X, \quad (124)$$

where $\Pi = c_s\alpha$, $X = -c_s^{-1}P_\alpha$ and we have introduced the sound wave frequency, ω, and coupling coefficient, g,

$$\omega = c_s|\mathbf{k}| = c_s(\mathcal{R}^{-2}k_x^2 + L_z^{-2}k_{\tilde{z}}^2)^{1/2}, \quad (125)$$

$$g = c_s\mathcal{R}^{-2}k_x k_{\tilde{z}}\frac{1 - (b/b_0)^{-2}}{\sqrt{k_x^2 b_0^2 + k_{\tilde{z}}^2}}. \quad (126)$$

There are two regimes depending on whether the waveperiod is short relative to $t_{\rm bg}$. When $\omega t_{\rm bg} \gg 1$ we have the WKB/modulated wave regime where the linear wave consists of a simple wave propagating on a slowly varying background. Taking ω as a large parameter, with $g = O(\omega^2)$, and provided $P_\beta = O(\omega^{-2})$ then the WKB solution for X is

$$X = X_\pm\omega^{-1/2}\exp\left(\pm i\int\omega d\tau\right). \quad (127)$$

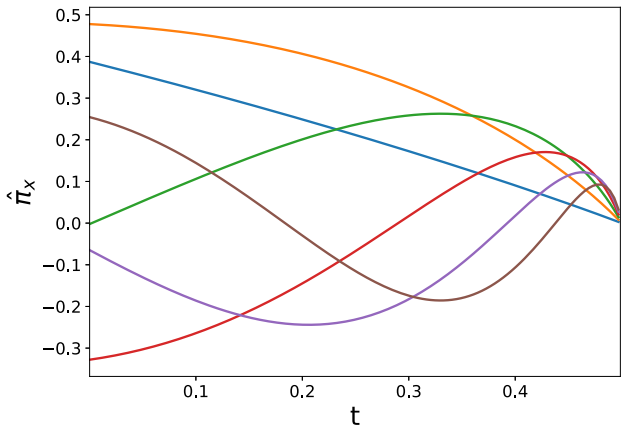

Figure 4. Amplitude (as measured by $\hat{\pi}_x$) of a horizontally propagating sound waves for a freely falling box with $\mathcal{R} = R_0(1 - t/t_c)^{2/3}$, $R_0 = 1$, $t_c = 0.5$, and wavenumbers $k_x = nc_{s0}^{-1}$, where n is an integer. The solutions correspond to Bessel functions (See Appendix B1). In the freeze out regime ($\omega t_{\rm bg} \lesssim 1$) the solution has no nodes on the time-scale of the collapse.

The WKB solution for α, P_α are then

$$\alpha \approx \pm i c_s^{-1}X_\pm\omega^{1/2}\exp\left(\pm i\int\omega d\tau\right), \quad (128)$$

$$P_\alpha \approx -c_s X_\pm\omega^{-1/2}\exp\left(\pm i\int\omega d\tau\right), \quad (129)$$

while P_β is a (small) constant. The WKB solutions, specifically equation (128) which is related to the density perturbation, show that if $\omega \to \infty$ at late times, for some choice of $k_x/k_{\tilde{z}}$ then there exists perturbations to the basic state (sound waves) which can grow to large amplitude. For horizontally propagating waves this corresponds to $\mathcal{R} \to 0$ (at late times), while for vertically propagating waves this is $L_z \to 0$. This condition is not sufficient, however, to determine if the non-linear saturation of such growing perturbations allows them to attain sufficient amplitude to affect the background flow.

In the opposite regime $\omega t_{\rm bg} \lesssim 1$ we have the freeze out regime where the wave phase cannot undergo a full cycle on the time-scale of the background flow and the wave becomes a roughly static pattern which is deformed by the background flow. These two regimes (modulated wave versus freeze out), seen in linear waves, has similarly been found for turbulence in contracting boxes (Robertson & Goldreich 2012), where a rapidly contracting box leads to an increase in the turbulent velocities on a time-scale too short for energy to be passed down the turbulent cascade.

A more detailed analysis of the linear waves in the local model is presented in Appendix B. Appendix B1 derives exact solutions for sound waves which are decoupled from the vortical wave (i.e. $g = 0$), for various background flows. Figs 4 and 5 show example solutions for horizontally propagating sound waves for free fall ($\mathcal{R} = R_0(1 - t/t_c)^{2/3}$) and uniform collapse ($\mathcal{R} = R_0 + U_0 t$) profiles respectively. In both cases the solution possesses no nodes on the time-scale of the collapse in the freeze out regime. The uniform collapse profile provides a useful illustration of the transition to the freeze out regime as P_α takes the form $P_\alpha \propto \mathcal{R}^{1/2\pm\lambda}$ where $\lambda = \frac{1}{2}\sqrt{1 - 4(c_S k_x/U_0)^2}$. For $k_x > \frac{1}{2}\frac{U_0}{c_s}$, λ is imaginary and we have a left and right propagating sound waves. While for $k_x < \frac{1}{2}\frac{U_0}{c_s}$, λ is real and the left and right sound waves are frozen out, becoming two non-propagating waves with differing growth rates.

Appendix B2 explores the diagonal linear waves (i.e. with $k_x, k_{\tilde{z}} \neq 0$) in more detail. Notably for diagonal waves the sound wave (P_α,

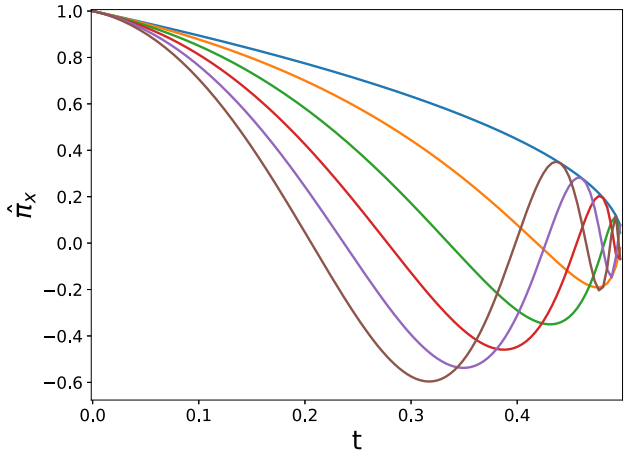

Figure 5. Amplitude of a horizontally propagating sound waves for a uniform collapse with $\mathcal{R} = R_0 + U_0 t, R_0 = 1, U_0 = 2$, and wavenumbers $k_x = nc_{s0}^{-1}$, where n is an integer. The solution corresponding to (complex) power laws. In the freeze out regime the power-law exponent is strictly real and there are no oscillations of the wave.

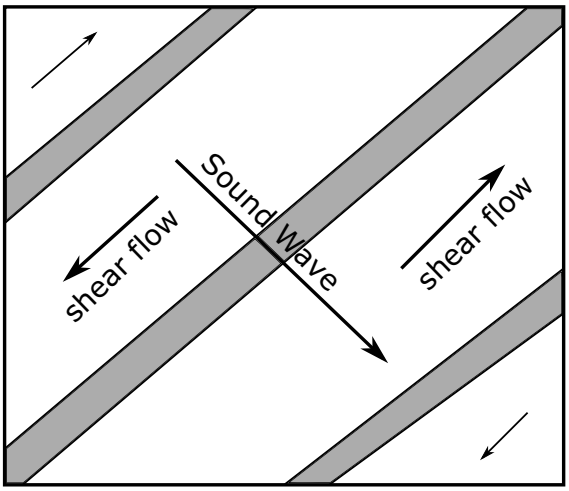

Figure 6. Cartoon illustrating the relationship between the diagonal sound waves and shear flows. The shear flow is generated parallel to the direction of the sound wave propagation. Likewise a diagonal shear flow will generate bands in the density running parallel to the shear flow as a result of exciting a standing sound wave.

α) and vortical waves (P_β, β) are coupled as a result of the changing aspect ratio of the box. This means a diagonally propagating sound wave will generate a shear flow perpendicular to the direction of wave propagation (illustrated in Fig. 6). Likewise an initially uniform density diagonal shear flow will generate a standing sound wave perpendicular to the fluid motion resulting in bands of varying density running parallel to the shear flow which arise. One complicating factor is in constant aspect ratio models, with $b \neq 1$, diagonally propagating sound waves, will produce shearing motions in the local model which are purely a result of the choice of coordinate system and do not represent physical shearing motions in the fluid. For numerical implementations, these sound wave generated shearing motions (either physical or as a result of the choice of coordinates) may present a challenge to some Riemann solvers.

In the global picture, the coupling occurs as a result of the advection of the background flow by the velocity perturbations in the diagonal waves. In many collapse profiles diagonal flows tend to become more horizontal with time. Thus one expects a weakly rotating collapse (which can be represented with a diagonal shear flow in the local model) to spontaneously generate tightly wound density waves at late times.

5 DISCUSSION

5.1 Implementing the local model in hydrocodes

The utility of a local model will be dependant on a practical numerical implementation. This has hindered the adoption of some local models in the past, notably the distorted shearing boxes with their time dependant geometries, and one is often left with the choice of attempting to coerce an existing code into running with an unusual geometry, or writing an entire specialized hydrocodes just for this specific application. These problems affects even relatively commonly used local models such as the regular shearing box, in particular with how to implement shear periodic boundaries. Examples of specific (magneto-)hydrodynamic codes being developed to model specific local model such as Paardekooper & Ogilvie (2019) for the warped shearing box, Wienkers & Ogilvie (2018) for the eccentric shearing box and Shi et al. (2020); Huang et al. (2022) for the expanding box. An alternative approach was pursued by Latter & Ogilvie (2006) and Ogilvie (2022) (for eccentric and warped disc, respectively) who instead made use of a regular shearing box but used a local representation of the distorted flow in setting up their model – which corresponds to the long wavelength part of the fluid flow on the box length-scale. This latter approach only works if the distorted and undistorted flows are similar enough that the distorted flow fits into the box (i.e. this works for linear warps/eccentricity). Appendix A presents several alternative formulations of the local model which may be useful for incorporating the model into existing hydrocodes.

5.2 On self-gravity in the local model

In this paper we have chosen not to consider self-gravity in our local model. It is worth noting that we have not made use of an explicit closure for the background gravitational potential Φ, which is only constrained to be spherically symmetric and varying on a length-scale much longer than L_H and L_V. Thus our local model is compatible with a self-gravitating background flow provided that the self-gravity of the density perturbations within the box can be ignored.

Looking ahead it seems likely one can include the self-gravity of the local flow by solving the Poisson's equation for the density difference $\rho - \rho_0$ subject to periodic boundaries. $\rho - \rho_0$ has zero mean, thus Poisson's equation can be inverted in Fourier space and the solutions likely correspond to the high degree spherical harmonics of the gravitational potential of the global problem. We leave demonstrating this, and exploring the effects of self-gravity, to future work.

5.3 Extensions

While interesting in it's own right, there are a number of useful generalizations to the local model that could be carried out. The obvious extension, given the close relationship between our model and the EBM/AEB, is to extend the model to include magnetic fields; likely following a similar approach to the MHD eccentric shearing box (Ogilvie & Barker 2014) rather than the approach of Tenerani & Velli (2017) for consistency with how we treat pressure. Regardless of the approach it is worth checking whether including

gradients in the background magnetic field (as done by Tenerani & Velli (2017)) will lead to spurious instabilities similar to gradients in the background pressure. We have chosen not to consider magnetic fields here in order to focus on the properties of the hydrodynamic model, particularly during collapse which has not been looked at before. Additionally, while adding magnetic fields to the local model in an expanding flow is straight forward, for a contracting flow one encounters additional complications. Magnetic fields in collapses are known to break spherical symmetry (Galli & Shu 1993; Hennebelle 2001; Galli et al. 2006) meaning one would need to make significant modifications to both the background flow and the resulting geometry of the local model to include them.

The second important generalization, particularly for realistic collapse profiles, is to include rotation in the background flow (such as Hennebelle 2001, 2003; Galli et al. 2006). As discussed in Section 3, slowly rotating collapses can already be modelled in our existing local model and take the form of growing, horizontal, shear flows in the local model. It should be obvious that faster rotating background flows will break spherical symmetry and, like with the inclusion of magnetic field, will necessitate a modification to the geometry of the local flow. If, however, such a generalization could be made to allow for the modelling differentially rotating collapses it would offer the possibility of following a collapse from it's initial nearly spherical cloud all the way to the formation of the disc, with the local model smoothly transitioning from that presented here for the initial collapse to the classic shearing box model at late times which provides a local mode for the newly formed disc.

Finally in the specific application of the local model to proto-planetary disc formation an important additional factor that would be useful to include is dust. If, as expected, the local model proves as as rich as the shearing box model in terms of the number of instabilities and other local phenomena then there should be ample opportunity for local flows with the collapse to concentrate dust – potentially jump starting planet formation by allowing the earliest stages of planet formation to occur prior to the disc being formed, in agreement with the detection of signposts of planet formation in very young stellar systems (Miotello et al. 2022; Tsukamoto et al. 2022).

6 CONCLUSION

In this paper, we have developed a local model for a spherically contracting/expanding gas cloud in the same vein as other local models which have achieved widespread usage in astrophysics and planetary science. The model consists of a periodic box with a Cartesian like, but time dependant geometry.

(i) The model is close to the accelerated EBM of Tenerani & Velli (2017), although we have a different treatment of pressure and density consistent with a small box limit. It is an extension of Robertson & Goldreich (2012) to allow for the non-isotropic expansion/contraction expected in spherical flows.

(ii) The model is spatially homogeneous allowing for the use of periodic (or shear-periodic) boundary conditions.

(iii) The model inherits a number of symmetries from fluid dynamics in periodic Cartesian domains and come from the global problem. Notably horizontal Galilean like transforms accelerate with time as consequence of conservation of angular momentum in the global problem.

(iv) The energy, density, and vorticity of the flow in the box all increase(/decrease) during the collapse(/expansion).

(v) We have derived several non-linear solutions to our local model. The most important of which are the horizontal shear flow, which correspond to zonal flows in the global problem. These shear flows grow in strength during a collapse as a consequence of conservation of angular momentum.

We have suggested several possible extensions to the local model. Our model will hopefully be of some use in the study of the early stages of disc/star formation. However the general utility of the local model will require the development of an effective numerical implementation.

ACKNOWLEDGEMENTS

We would like to thank Benoît Commerçon, Matthew Kunz, and Pascal Wang for invaluable help with the literature; Ziyan Xu and Timothée Cléris for discussion pertaining to requirements for numerical implementations and Francesco Lovascio for useful discussions/sanity checking some of the more unexpected properties of the model. We thank the reviewer for there suggestions which helped improve the clarity of this paper.

EL would like to thank the European Research Council (ERC). This research was supported by the ERC through the CoG project PODCAST Number 864965. This project has received funding from the European Union's Horizon 2020 research and innovation programme under the Marie Skłodowska-Curie grant agreement number 823823.

7 DATA AVAILABILITY

No new data were generated or analysed in support of this research.

REFERENCES

Balbus S. A., Ricotti M., 1999, ApJ, 518, L784
Baumann D., Nicolis A., Senatore L., Zaldarriaga M., 2012, J. Cosmol. Astropart. Phys., 2012, 051
Bethe H. A., Fuchs K., Hirschfelder J. O., Magee J. L., Neumann R. v., 1958, Technical Report, Blast Wave. Los Alamos National Lab, Los Alamos, NM
Bondi H., 1952, MNRAS, 112, 195
Dewberry J. W., Latter H. N., Ogilvie G. I., 2019, MNRAS, 483, 1609
Dewberry J. W., Latter H. N., Ogilvie G. I., Fromang S., 2020, MNRAS, 497, 451
Foster P. N., Chevalier R. A., 1993, ApJ, 416, L303
Galli D., Shu F. H., 1993, ApJ, 417, L220
Galli D., Lizano S., Shu F. H., Allen A., 2006, ApJ, 647, L374
Goldreich P., Lynden-Bell D., 1965, MNRAS, 130, 125
Grappin R., Velli M., 1996, J. Geophys. Res., 101, 425
Grappin R., Velli M., Mangeney A., 1993, Phys. Rev. Lett., 70, 2190
Hawley J. F., Gammie C. F., Balbus S. A., 1995, ApJ, 440, L742
Hennebelle P., 2001, A&A, 378, 214
Hennebelle P., 2003, A&A, 411, 9
Hernandez X., Nasser L., Aguayo-Ortiz A., 2023, ApJ, 945, 76
Huang Z., Shi C., Velli M., Sioulas N., 2022, ApJ, 935, 60
Hunter C., 1977, ApJ, 218, L834
Larson R. B., 1969, MNRAS, 145, 271
Latter H. N., Ogilvie G. I., 2006, MNRAS, 372, 1829
Latter H. N., Papaloizou J., 2017, MNRAS, 472, 1432
Lynden-Bell D., Ostriker J. P., 1967, MNRAS, 136, 293
Miotello A., Kamp I., Birnstiel T., Cleeves L. I., Kataoka A., 2022, preprint (arXiv:2203.09818)
Mo H., Van den Bosch F., White S., 2010, Galaxy Formation and Evolution, 1st edn. Cambridge Univ. Press, New York
Ogilvie G. I., 2022, MNRAS, 513, 1701

Ogilvie G. I., Barker A. J., 2014, MNRAS, 445, 2621
Ogilvie G. I., Latter H. N., 2013, MNRAS, 433, 2403
Paardekooper S.-J., Ogilvie G. I., 2019, MNRAS, 483, 3738
Padhye N., Morrison P. J., 1996, Plasma Phys. Rep., 22, 10
Papaloizou J. C. B., 2005, A&A, 432, 743
Penston M. V., 1969, MNRAS, 144, 425
Robertson B., Goldreich P., 2012, ApJ, 750, L31
Rossby C.-G., 1939, J. Mar. Res., 2, 38
Sedov L. I., 1946, J. Appl. Math. Mech., 10, 241
Shi C., Velli M., Tenerani A., Rappazzo F., Réville V., 2020, ApJ, 888, L68
Shu F. H., 1977, ApJ, 214, L488
Taylor G. I., 1946, Proc. Royal Society of London. Series A. Mathematical and Physical Sciences, 186, 273
Taylor G., 1950, Proc. Royal Society of London. Series A, Mathematical and Physical Sciences, 201, 159
Tenerani A., Velli M., 2017, ApJ, 843, L26
Tsukamoto Y., et al., 2022, preprint (arXiv:2209.13765)
Velli M., Grappin R., Mangeney A., 1992, in Spicer D. S., MacNeice P., eds, AIP Conf. Proc. Vol. 267, Electromechanical Coupling of the Solar Atmosphere. Am. Inst. Phys., New York, p. 154
Wienkers A. F., Ogilvie G. I., 2018, MNRAS, 477, 4838

APPENDIX A: REFORMULATED EQUATIONS FOR EASIER NUMERICAL IMPLEMENTATION

An issue faced by our local model, which it shares with the distorted shearing box models (e.g. Ogilvie & Latter 2013; Ogilvie & Barker 2014), is how to include the time dependant geometry in existing solvers. This has hindered the implementation of local models in the past and has led to workarounds such as Latter & Ogilvie (2006) and Ogilvie (2022). In this appendix we derive various (equivalent) alternative formalism for the local model that may facilitate its implementation in existing hydrocodes.

A1 Modified continuity equations

The momentum equation can be written in Cartesian like geometry which removes the time dependant terms in front of the derivatives, by use of an asymmetric stress tensor T_{ij},

$$Dv^x + \frac{2U_0}{\mathcal{R}}v^x = \frac{1}{\rho}\partial_x T^{xx}, \tag{A1}$$

$$Dv^y + \frac{2U_0}{\mathcal{R}}v^y = \frac{1}{\rho}\partial_y T^{yy}, \tag{A2}$$

$$Dv^{\bar{z}} + 2v^{\bar{z}}U_{R0} = \frac{1}{\rho}\partial_{\bar{z}} T^{\bar{z}\bar{z}}, \tag{A3}$$

where

$$T^{xx} = T^{yy} = -\frac{p}{\mathcal{R}^2}, \quad T^{\bar{z}\bar{z}} = -\frac{p}{L_z^2}, \quad T^{xy} = T^{x\bar{z}} = T^{y\bar{z}} = 0. \tag{A4}$$

One way to interpret this tensor is as an anisotropic sound speed with sound waves propagating at different speeds in the horizontal and vertical directions. Alternatively we can interpret this as a modified equation of state with stresses from pseudo-self-gravity or pseudo-magnetic field based on the following stress tensor for a self-gravitating, ideal MHD fluid,

$$T^{ij} = -p'\delta^{ij} - \frac{1}{4\pi G}\left(g^i g^j - \frac{1}{2}g^2\delta^{ij}\right) + \frac{1}{\mu_0}\left(B^i B^j - \frac{1}{2}B^2\delta^{ij}\right). \tag{A5}$$

Substituting the expressions for the stress tensor components into the above expression we see that we require $g^x = g^y = B^x = B^y = 0$ in order that the cross terms, T^{xy}, $T^{x\bar{z}}$ and $T^{y\bar{z}}$ vanish. Adding $T^{xx} + T^{\bar{z}\bar{z}}$ (or equivalently $T^{yy} + T^{\bar{z}\bar{z}}$) we arrive at an expression relating the old pressure, p, to the new pressure, p',

$$p' = \frac{1}{2}\left(\frac{1}{\mathcal{R}^2} + \frac{1}{L_z^2}\right)p. \tag{A6}$$

Subtracting $T^{xx} - T^{\bar{z}\bar{z}}$ (equivalently $T^{yy} - T^{\bar{z}\bar{z}}$) we obtain the anisotropic part of the stress which is independent of p'. When $L_z \geq \mathcal{R}$ we can interpret this as a vertical field

$$B^{\bar{z}} = \sqrt{\mu_0 p}\left(\frac{1}{\mathcal{R}^2} - \frac{1}{L_z^2}\right)^{1/2}, \tag{A7}$$

with $g^{\bar{z}} = 0$. While if $\mathcal{R} \geq L_z$ we can instead interpret this as a vertical self-gravitational acceleration,

$$g^{\bar{z}} = \sqrt{4\pi G p}\left(\frac{1}{L_z^2} - \frac{1}{\mathcal{R}^2}\right)^{1/2}, \tag{A8}$$

with $B^{\bar{z}} = 0$. Note that that neither of these are real magnetic or self-gravity fields as they do not evolve in the correct way, or have the appropriate properties. For example the pseudo-magnetic field given by equation (A7) is not, typically, divergence free.

For more general spherical flows where these inequalities cannot be guaranteed we can instead include a mixture of effective vertical self-gravitating acceleration of the following form,

$$B^{\bar{z}} = \sqrt{\mu_0 p}\mathcal{R}^{-1}, \tag{A9}$$

$$g^{\bar{z}} = \sqrt{4\pi G p}L_z^{-1}. \tag{A10}$$

A2 Relative density

For many numerical implementations (particularly Lagrangian/Particle based methods) it is preferable that there is no modification to the continuity equation. One can achieve this, for certain equations of state, by rewriting the continuity equation in terms of the relative density $\psi = \rho/\rho_{\rm ref}$ such that

$$D\psi = -\psi \partial_i v^i. \tag{A11}$$

The reference density is that of the basic state with $\rho_{\rm ref} = \rho_{\rm ref}(\tau)$, which evolves according to

$$D\rho_{\rm ref} = -\rho_{\rm ref}\Delta. \tag{A12}$$

Assuming the equation of state is polytropic, and takes the form $p = K(x, y, z)\rho^{1+1/n}$, which is appropriate for both adiabatic ($1 + 1/n = \gamma$) and locally isothermal ($n \to \infty$) equations of state, then we can rewrite the equation of state in terms of the relative density by introducing the reference pressure $p_{\rm ref}(x, y, z, t) = K(x, y, z)\rho_{\rm ref}^{1+1/n}$. The equation of state is then $p = p_{\rm ref}\psi^{1+1/n}$. The fluid equations are then

$$Dv^x + \frac{2U_0}{\mathcal{R}}v^x = -\frac{1}{\psi\mathcal{R}^2}\partial_x(p/\rho_{\rm ref}), \tag{A13}$$

$$Dv^y + \frac{2U_0}{\mathcal{R}}v^y = -\frac{1}{\psi\mathcal{R}^2}\partial_y(p/\rho_{\rm ref}), \tag{A14}$$

$$Dv^{\tilde{z}} + 2v^{\tilde{z}}U_{R0} = -\frac{1}{\psi L_z^2}\partial_{\tilde{z}}(p/\rho_{\rm ref}), \tag{A15}$$

$$D\psi = -\psi\left[\partial_x v^x + \partial_y v^y + \partial_{\tilde{z}} v^{\tilde{z}}\right]. \tag{A16}$$

These equations can be derived from the following Lagrangian

$$L = \int \psi\left[\frac{1}{2}\mathcal{R}^2\left(v^x v^x + v^y v^y\right) + \frac{1}{2}L_z v^{\tilde{z}} v^{\tilde{z}} - n\frac{p_{\rm ref}}{\rho_{\rm ref}}\psi^{1/n}\right] dx\, dy\, d\tilde{z}, \tag{A17}$$

which is useful for deriving smooth particle hydrodynamics base methods. The main difference between this Lagrangian and the more commonly used Lagrangian for ideal fluid is the presence of the time dependant coefficients, $\mathcal{R}$, L_z, $p_{\rm ref}$, and $\rho_{\rm ref}$.

APPENDIX B: ANALYSIS OF THE LINEAR WAVES

B1 Exact solutions for sound waves when decoupled from the vortical waves

For many simple spherical flows it is possible to obtain exact solutions for sound waves when they are decoupled from the vortical wave (i.e. with a coupling coefficient $g = 0$). This occurs for both purely horizontal and purely vertical waves, along with background flow with a constant aspect ratio (the situation considered in cosmological fluids). To describe the background flow we consider various functional forms for the reference length-scale $L = L(\tau)$ and obtain solutions for the sound waves in the local model. We adopt

$$L = L_0\frac{|\mathbf{k}_0|}{|\mathbf{k}|} = L_0\frac{\mathcal{R}}{\mathcal{R}_0}\left(\frac{k_x^2 + b_0^{-2}k_{\tilde{z}}^2}{k_x^2 + b^{-2}k_{\tilde{z}}^2}\right)^{1/2}, \tag{B1}$$

as our reference length-scale, where $|\mathbf{k}|$ denotes the magnitude of the wavevector and $|\mathbf{k}_0|$ is the initial $|\mathbf{k}|$. For a horizontally propagating wave choosing $L_0 = R_0$ results in $L = \mathcal{R}$. Similarly for vertically propagating waves, $L_0 = L_{z0}$ results in $L = L_z$. Finally for a constant aspect ratio ($b = b_0$) the reference length can be identified with the scale factor a.

We consider two forms of power-law profiles, given by

$$L = L_0(\tau/\tau_{\rm c})^{\beta}, \tag{B2}$$

$$L = L_0(1 - \tau/\tau_{\rm c})^{\beta}, \tag{B3}$$

the latter includes the linear/uniform collapse/expansion when $\beta = 1$. On can also consider an exponential collapse/expansion,

$$L = L_0\exp(H\tau), \tag{B4}$$

where H is a constant Hubble parameter. The exponential profile can be obtained from equation (B3) by taking $\tau_c = -H^{-1}\beta$ and taking the limit $\beta \to \infty$. A logarithmic profile can be similarly obtained by setting $L_0 = A\beta$, for some constant A, and taking the limit $\beta \to 0$. Finally, although we shall not explicitly obtain sound wave solutions for it, the early stages of the isothermal sphere model of Shu (1977) leads to the background radius evolving according to

$$\mathcal{R}^2 = L^2 = L_0^2\left[1 - (\tau/\tau_c)^2\right]. \tag{B5}$$

The dynamics of the sound wave, when it is decoupled from the vortical wave, can be obtained from the following Hamiltonian:

$$\mathcal{H} = \frac{1}{2}c_s^{-2}\omega^2(\tau)P_\alpha^2 + \frac{1}{2}c_s^2\alpha^2, \tag{B6}$$

where $\omega(\tau) = c_s|\mathbf{k}_0|L_0/L$ is the sound wave frequency. This equation can be obtained from equation (123) by setting the coupling term, $c_s^{-1}g(\tau)P_\alpha P_\beta$, to zero. Hamilton's equations lead to

$$\partial_\tau P_\alpha = -c_s^2 \alpha, \tag{B7}$$

$$\partial_\tau \alpha = c_s^{-2} \omega^2 P_\alpha, \tag{B8}$$

from which we obtain the following, parametric oscillator, equation for the momentum:

$$\partial_\tau^2 P_\alpha + \omega^2 P_\alpha = 0. \tag{B9}$$

For both the power-law profiles the evolutionary equation for the momentum is

$$\partial_\tau^2 P_\alpha + \omega_0^2 s^{-2\beta/\alpha} P_\alpha = 0, \tag{B10}$$

where $\omega_0 = c_s|\mathbf{k}|(\tau_0/\tau_c)^{-\beta}$ and we have introduced s which for the equation (B2) is given by $s = (\tau/\tau_0)^\alpha$ and for equation (B3) is given by $s = (\frac{\tau_c - \tau}{\tau_0})^\alpha$. In both cases this leads to the reference length-scale taking the form $L = L_0(\tau_0/\tau_c)^\beta s^{\beta/\alpha}$. The characteristic time-scale relevant to this, $t_{\rm bg} = L/|\dot{L}|$, is given by

$$t_{\rm bg} = \frac{\tau_0 s^{1/\alpha}}{|\beta|}, \tag{B11}$$

by setting $\omega t_{\rm bg} = 1$, and writing in terms of L, we can calculate the reference length-scale at freeze out (provided $\beta \neq 1$),

$$L_{\rm freezeout} = L_0 \left(\frac{\tau_0}{\tau_c}\right)^\beta \left(\frac{|\beta|}{\omega_0 \tau_0}\right)^{\beta/(1-\beta)}, \tag{B12}$$

which gives the value of L at which a mode of a given wavelength enters (or exits) the freeze out regime. Equation (B10) can be transformed into Bessel's equation by setting $P_\alpha = A s^\lambda f(s)$, resulting in the following equation for f,

$$s^2 f''(s) + [1 - 1/\alpha + 2\lambda] s f'(\tau) + \left[\lambda(\lambda - 1/\alpha) + \omega_0^2 \alpha^{-2} \tau_0^2 s^{2(1-\beta)/\alpha}\right] f(\tau) = 0, \tag{B13}$$

where we have made use of $\ddot{s} s \dot{s}^{-2} = 1 - 1/\alpha$ and $\dot{s}^2 = \alpha^2 \tau_0^{-2} s^{2-2/\alpha}$.

For $\beta \neq 1$, equation (B13) corresponds to Bessel's equation provided that $\alpha = 1 - \beta$, $\lambda = \frac{1}{2(1-\beta)}$ and

$$\tau_0 = \left[\frac{|1-\beta|}{c_s |\mathbf{k}_0| \tau_c^\beta}\right]^{1/(1-\beta)}, \tag{B14}$$

This results in the following general solution for P_α,

$$P_\alpha = s^{1/[2(1-\beta)]} \left[A J_\nu(s) + B Y_\nu(s)\right], \tag{B15}$$

where J_ν and Y_ν are Bessel functions with order $\nu = \frac{1}{2|1-\beta|}$. The solution for the exponential profile can be obtained from the above by taking the limit $\beta \to \infty$. This can, alternatively, be written in terms of the reference length,

$$P_\alpha = L^{1/(2\beta)} \left\{ \tilde{A} J_\nu \left[\left|\frac{1-\beta}{\beta}\right| \left(\frac{L}{L_{\rm freezeout}}\right)^{(1-\beta)/\beta}\right] + \tilde{B} Y_\nu \left[\left|\frac{1-\beta}{\beta}\right| \left(\frac{L}{L_{\rm freezeout}}\right)^{(1-\beta)/\beta}\right] \right\}, \tag{B16}$$

where the freeze out radius can be simplified to

$$L_{\rm freezeout} = L_0 \left(\frac{\tau_0}{\tau_c}\right)^\beta \left|\frac{\beta}{1-\beta}\right|^{\beta/(1-\beta)}, \tag{B17}$$

and we have absorbed constant terms into $\tilde{A}$ and $\tilde{B}$. In terms of the s variable the velocity and density perturbations, due to the sound wave, are

$$\delta v^x = \frac{2k_x}{\mathcal{R}^2} s^{1/[2(1-\beta)]} \left\{\mathrm{Re}[A \exp(i\mathbf{k}\cdot\mathbf{x})] J_\nu(s) + \mathrm{Re}[B \exp(i\mathbf{k}\cdot\mathbf{x})] Y_\nu(s)\right\}, \tag{B18}$$

$$\delta v^{\tilde{z}} = \frac{2k_{\tilde{z}}}{L_z^2} s^{1/[2(1-\beta)]} \left\{\mathrm{Re}[A \exp(i\mathbf{k}\cdot\mathbf{x})] J_\nu(s) + \mathrm{Re}[B \exp(i\mathbf{k}\cdot\mathbf{x})] Y_\nu(s)\right\}, \tag{B19}$$

$$\delta\rho = -\frac{2\rho}{c_s^2} \frac{1-\beta}{\tau_0} s^{\frac{1-2\beta}{2(1-\beta)}} \mathrm{sgn}(\dot{s}) \left\{\mathrm{Im}[A \exp(i\mathbf{k}\cdot\mathbf{x})] J_{\nu-1}(s) + \mathrm{Im}[B \exp(i\mathbf{k}\cdot\mathbf{x})] Y_{\nu-1}(s)\right\}. \tag{B20}$$

These solutions are very similar to linear perturbation to FRW-cosmology in the presence of a perfect fluid (e.g. see Baumann et al. (2012)). This similarity is mostly a reflection of the similar mathematical structure (2nd-order linear differential equations with power-law coefficients). In both cases the background is a spatially homogeneous perfect fluid in an FRW-(like) metric. In our local model we consider perturbations to the fluid holding the metric fixed. In cosmological perturbation theory, however, one is instead considering perturbations to the metric in the presence of the fluid.

The above solutions work for $\beta \neq 1$. For $\beta = 1$ the above solution is singular as $\nu \to \infty$. Without loss of generality we can set $\alpha = 1$ and one sets $\lambda = 0$ leading to

$$s^2 f'' + (c_s |\mathbf{k}_0| \tau_c)^2 f = 0. \tag{B21}$$

This can be solved by setting $f = s^\gamma$, provided

$$\gamma(\gamma - 1) = -(c_s |\mathbf{k}_0| \tau_c)^2, \tag{B22}$$

resulting in the general solution

$$P_\alpha = \sqrt{s}\left[A_+ s^\lambda + A_- s^{-\lambda}\right], \tag{B23}$$

where we have introduced $\lambda = \frac{1}{2}\sqrt{1-4\,(c_s|\mathbf{k}_0|\tau_c)^2}$ In terms of the reference length-scale the solution is

$$P_\alpha = \sqrt{L}\left[\tilde{A}_+ L^\lambda + \tilde{A}_- L^{-\lambda}\right], \tag{B24}$$

where, again, we have absorbed constant terms into $\tilde{A}_+$ and $\tilde{A}_-$. From this expression we can obtain the following density and velocity perturbations

$$\delta v^x = \frac{2}{\mathcal{R}^2} k_x \sqrt{L}\left\{\mathrm{Re}\left[\tilde{A}_+ L^\lambda \exp\left(i\mathbf{k}\cdot\mathbf{x}\right)\right] + \mathrm{Re}\left[\tilde{A}_- L^{-\lambda} \exp\left(i\mathbf{k}\cdot\mathbf{x}\right)\right]\right\}, \tag{B25}$$

$$\delta v^{\tilde{z}} = \frac{2}{L_z^2} k_{\tilde{z}} \sqrt{L}\left\{\mathrm{Re}\left[\tilde{A}_+ L^\lambda \exp\left(i\mathbf{k}\cdot\mathbf{x}\right)\right] + \mathrm{Re}\left[\tilde{A}_- L^{-\lambda} \exp\left(i\mathbf{k}\cdot\mathbf{x}\right)\right]\right\}, \tag{B26}$$

$$\delta\rho = \frac{2\rho L_0}{c_s^2 \tau_c} L^{-1/2}\left\{\mathrm{Im}\left[(\lambda+1/2)\,\tilde{A}_+ L^\lambda \exp\left(i\mathbf{k}\cdot\mathbf{x}\right)\right] - \mathrm{Im}\left[(\lambda-1/2)\,\tilde{A}_- L^{-\lambda} \exp\left(i\mathbf{k}\cdot\mathbf{x}\right)\right]\right\}. \tag{B27}$$

This solution is useful to illustrate the effects of freeze-out on the wave. For large $|\mathbf{k}_0|$, λ is imaginary and the $+$ and $-$ solutions corresponds to left and right travelling waves which grow during a collapse. Reducing $|\mathbf{k}_0|$ induces a phase shift between the density and velocity perturbation. When $|\mathbf{k}_0|$ drops below $k_{\mathrm{freezeout}} = \frac{1}{2c_s\tau_c}$ then the wave enters the freeze-out regime where the left and right travelling waves become standing waves with differing growth(/decay)-rates.

Solutions for horizontally propagating sound waves in the isothermal sphere collapse of Shu (1977) (equation (B5)) can similarly be found in terms of Hypergeomtric functions, however we shall not do this here.

B2 Diagonally propagating waves and sound wave-vortical wave coupling

The density and velocity perturbations with wavenumber $\pm\mathbf{k}$ can be obtained from the (α, β, γ, P_α, P_β, P_γ) system of coordinates and momenta as follows

$$\delta v^x = \frac{2}{\mathcal{R}^2}\left\{k_x \mathrm{Re}\left[P_\alpha \exp(i\mathbf{k}\cdot\mathbf{x})\right] + \frac{k_{\tilde{z}}}{\sqrt{k_x^2 b_0^2 + k_{\tilde{z}}^2}}\mathrm{Re}\left[P_\beta \exp(i\mathbf{k}\cdot\mathbf{x})\right]\right\}, \tag{B28}$$

$$\delta v^y = \frac{2}{\mathcal{R}^2}\,\mathrm{Re}\left[P_\gamma \exp(i\mathbf{k}\cdot\mathbf{x})\right] \tag{B29}$$

$$\delta v^{\tilde{z}} = \frac{2}{L_z^2}\left\{k_{\tilde{z}} \mathrm{Re}\left[P_\alpha \exp(i\mathbf{k}\cdot\mathbf{x})\right] - \frac{k_x b_0^2}{\sqrt{k_x^2 b_0^2 + k_{\tilde{z}}^2}}\mathrm{Re}\left[P_\beta \exp(i\mathbf{k}\cdot\mathbf{x})\right]\right\}, \tag{B30}$$

$$\delta\rho = 2\rho\,\mathrm{Im}\left[\alpha \exp\left(i\mathbf{k}\cdot\mathbf{x}\right)\right], \tag{B31}$$

where we have made use of the reality of the perturbations where we require $\delta\mathbf{v}^* = \delta\mathbf{v}$ and $\delta\rho^* = \delta\rho$. P_β and P_γ are integrals of motion related to the fluid vorticity. The dynamics of the (α, P_α)are obtained from the following Hamiltonian,

$$\mathcal{H} = \frac{1}{2}c_s^{-2}\omega^2(\tau)P_\alpha^2 + c_s^{-1}g(\tau)P_\alpha P_\beta + \frac{1}{2}c_s^2\alpha^2, \tag{B32}$$

where the sound wave frequency, ω, and coupling coefficient, g, are given by equations (125) and (126), respectively.

Neglecting P_γ we have the following WKB solutions for $\delta\rho$ and $\delta\mathbf{v}$,

$$\delta v^x \approx -\frac{2c_s}{\mathcal{R}^2}\omega^{-1/2}k_x \mathrm{Re}\left[X_+ \exp\left(i\mathbf{k}\cdot\mathbf{x} + i\int\omega d\tau\right) + X_- \exp\left(i\mathbf{k}\cdot\mathbf{x} - i\int\omega d\tau\right)\right] + \frac{2}{\mathcal{R}^2}\frac{k_{\tilde{z}}}{\sqrt{k_x^2 b_0^2 + k_{\tilde{z}}^2}}\mathrm{Re}\left[P_\beta \exp\left(i\mathbf{k}\cdot\mathbf{x}\right)\right] \tag{B33}$$

$$\delta v^{\tilde{z}} \approx -\frac{2c_s}{L_z^2}\omega^{-1/2}k_z \mathrm{Re}\left[X_+ \exp\left(i\mathbf{k}\cdot\mathbf{x} + i\int\omega d\tau\right) + X_- \exp\left(i\mathbf{k}\cdot\mathbf{x} - i\int\omega d\tau\right)\right] - \frac{2}{L_z^2}\frac{k_x b_0^2}{\sqrt{k_x^2 b_0^2 + k_{\tilde{z}}^2}}\mathrm{Re}\left[P_\beta \exp\left(i\mathbf{k}\cdot\mathbf{x}\right)\right] \tag{B34}$$

$$\delta\rho \approx \frac{2\rho}{c_s}\omega^{1/2}\mathrm{Re}\left[X_+ \exp\left(i\mathbf{k}\cdot\mathbf{x} + i\int\omega d\tau\right) - X_- \exp\left(i\mathbf{k}\cdot\mathbf{x} - i\int\omega d\tau\right)\right], \tag{B35}$$

with $\delta v^y = 0$ and $X_\pm$ and P_β are (complex) constants. For diagonally propagating waves we require $|P_\beta| \ll c_s\omega^{-1/2}|X_\pm|$ in order for the above approximation to be valid.

It is useful to consider the shear and velocity divergence as a result of the linear waves. The divergence of the velocity is given by

$$\partial_i \delta v^i = \frac{2}{\mathcal{R}^2}\left(k_x^2 + b^{-2}k_{\tilde{z}}^2\right)\mathrm{Re}[i\,P_\alpha \exp\left(i\mathbf{k}\cdot\mathbf{x}\right)] + \frac{2}{\mathcal{R}^2}\frac{k_x k_{\tilde{z}}}{\sqrt{k_x^2 b_0^2 + k_{\tilde{z}}^2}}\left[1-(b/b_0)^{-2}\right]\mathrm{Re}[i\,P_\beta \exp\left(i\mathbf{k}\cdot\mathbf{x}\right)], \tag{B36}$$

while the velocity shear (neglecting δv^y) can be characterized by

$$k_{\tilde{z}}\delta v^x - k_x \delta v^{\tilde{z}} = \frac{2}{\mathcal{R}^2}\left\{k_x k_{\tilde{z}}(1-b^{-2})\mathrm{Re}[P_\alpha \exp(i\mathbf{k}\cdot\mathbf{x})] + \frac{k_x^2 b^2 + k_{\tilde{z}}^2}{\sqrt{k_x^2 b_0^2 + k_{\tilde{z}}^2}}\mathrm{Re}[P_\beta \exp(i\mathbf{k}\cdot\mathbf{x})]\right\}. \tag{B37}$$

Diagonal vortical waves, with $P_\alpha(0) = \alpha(0) = 0$, cause a divergence of the velocity (and thus a density perturbation) when the coupling coefficient $g \neq 0$. This occurs as a result of a varying box aspect ratio. Similarly, from equation (B37), we see that diagonal sound waves (with $P_\beta = 0$) generate a shear flow perpendicular to the direction of propagation if the aspect ratio $b \neq 1$. For a constant aspect ratio ($b = b_0$) this is simply a consequence of the choice of coordinate system and does not reflect a physical shear in the fluid flow. However, when the aspect ratio is time dependant this shear cannot be removed by a suitable rescaling of the coordinates, meaning the propagating sound waves can generate velocity shear in flows with a time varying b.

APPENDIX C: LOCAL MODELS OF SOME ANALYTICAL BACKGROUND FLOWS

In this section we shall consider some example spherical flows and show how to obtain the geometrical coefficients necessary to formulate the local model. A wide variety of spherical problems can be described by power-law flows of the form

$$U = \mathcal{U}_0 (R/R_0)^\beta, \tag{C1}$$

where $\mathcal{U}_0$, R_0, and β are constants, over some range of radii. This includes the free-fall case $\beta = -1/2$, the Penston (1969) solution away from the transition point ($\beta = 1/7$ at large R and $\beta = 1/2$ at small R) and the solution of Hernandez, Nasser & Aguayo-Ortiz (2023) ($\beta = -1/2$). Steady flows require $\rho_0 \propto R^{-(2+\beta)}$, however the local model is agnostic to whether the flow is a steady state.

We shall also consider the isothermal spherical collapse problem due to Shu (1977). This has a radial velocity at large radii/early times of

$$U = -a^2 (A-2) t R^{-1}. \tag{C2}$$

where a and A have the same meaning as in Shu (1977).

Starting with the power-law flow. The reference radius can be obtained from

$$\dot{\mathcal{R}} = U(\mathcal{R}) = \mathcal{U}_0 R_0^{-\beta} \mathcal{R}^\beta, \tag{C3}$$

which has solution

$$\mathcal{R} = R_0 \left[1 + (1-\beta)\mathcal{U}_0 R_0^{-1} t\right]^{1/(1-\beta)}. \tag{C4}$$

This allows us to determine U_0 and U_{R0},

$$U_0 = U(\mathcal{R}) = \mathcal{U}_0 \left[1 + (1-\beta)\mathcal{U}_0 R_0^{-1} t\right]^{\beta/(1-\beta)}, \tag{C5}$$

$$U_{R0} = \left.\frac{\partial U}{\partial R}\right|_{R=\mathcal{R}} = \beta \mathcal{U}_0 R_0^{-1} \left[1 + (1-\beta)\mathcal{U}_0 R_0^{-1} t\right]^{-1}. \tag{C6}$$

Substituting the expression for U_{R0} into the evolutionary equation for L_z, $\dot{L}_z = U_{R0} L_z$, we obtain an expression for L_z

$$L_z = L_{z0} \left[1 + (1-\beta)\mathcal{U}_0 R_0^{-1} t\right]^{\beta/(1-\beta)}, \tag{C7}$$

with L_{z0} the initial vertical length-scale. The divergence of the background flow, Δ, is then

$$\Delta = (2+\beta)\mathcal{U}_0 R_0^{-1} \left[1 + (1-\beta)\mathcal{U}_0 R_0^{-1} t\right]^{-1}. \tag{C8}$$

The basic state for this model is $v = 0$ and a spatially homogeneous density given by

$$\rho = \rho_{\rm init} \left[1 + (1-\beta)\mathcal{U}_0 R_0^{-1} t\right]^{-(2+\beta)/(1-\beta)}, \tag{C9}$$

where $\rho_{\rm init}$ is the initial density.

For the model of Shu (1977) we can similarly obtain an expression for $\mathcal{R}$,

$$\mathcal{R} = R_0 \left[1 - \frac{a^2}{R_0^2}(A-2)t^2\right]^{1/2}. \tag{C10}$$

We thus obtain expressions for U_0 and U_{R0},

$$U_0 = -a^2 (A-2) R_0^{-1} t \left[1 - \frac{a^2}{R_0^2}(A-2)t^2\right]^{-1/2}, \quad U_{R0} = \frac{a^2}{R_0^2}(A-2)t \left[1 - \frac{a^2}{R_0^2}(A-2)t^2\right]^{-1}. \tag{C11}$$

From these we obtain expressions for L_z,

$$L_z = L_{z0} \left[1 - \frac{a^2}{R_0^2}(A-2)t^2\right]^{-1/2}, \tag{C12}$$

while the divergence of the background flow is

$$\Delta = -\frac{a^2}{R_0^2}(A-2)t \left[1 - \frac{a^2}{R_0^2}(A-2)t^2\right]^{-1}. \tag{C13}$$

The basic state of the local model for the Shu (1977) isothermal collapse is $v = 0$ and a spatially homogeneous density given by

$$\rho = \rho_{\rm init} \left[1 - \frac{a^2}{R_0^2}(A-2)t^2\right]^{-1/2}. \tag{C14}$$

This appendix has shown how to go from fairly simple collapse profiles (power law and the isothermal sphere model) to the geometrical terms necessary to formulate the local model. More general global collapse solutions can only be obtained numerically meaning there will be no closed form solution for the geometric terms. However, the principles of obtaining the geometric terms remain the same and can be expressed as numerical solutions to the ODEs $\dot{\mathcal{R}} = U_0(\mathcal{R}, t)$ and $\dot{L}_z = U_{R0} L_z$.

This paper has been typeset from a TEX/LATEX file prepared by the author.